Oscillations in Monotone Systems with a Negative Feedback*

Tomáš Gedeon†

Abstract. We study a finite-dimensional monotone system coupled to a slowly evolving scalar differential equation which provides a negative feedback to the monotone system. We use a theory of multivalued characteristics to show that this system admits a relaxation periodic orbit if a simple model system in $\mathbf{R}^2$ does. Our construction can be used to prove the existence of periodic orbits in slow-fast systems of arbitrary dimension. We apply our theory to a model of a cell cycle in *Xenopus* embryos. Abrupt changes in signals upon entry to mitosis suggests that the cell cycle is generated by a relaxation oscillation. Our results show that the cell cycle orbit is not a relaxation oscillator. However, we construct a closely related system that exhibits relaxation oscillations and that approximates the cell cycle oscillator for an intermediate range of negative feedback strengths. We show that the cell cycle oscillation disappears if the negative feedback is too weak or too strong.

1. Introduction. Genetic networks that support bistable [28, 33, 17, 5, 6, 34, 31] and periodic [11] behaviors have attracted much attention in recent years. Bistable systems are thought to be involved in the generation of switch-like biochemical responses [17, 5] as well as in the establishment of cell cycle oscillations and mutually exclusive cell cycle phases [34, 31]. Biologically, relaxation oscillators appear to underlie many important cell processes, such as the early embryonic cell cycle in frog eggs (*Xenopus* oocytes) [34, 31, 29, 37]. There are other recognized mechanisms, most notably a delayed negative feedback [22, 36, 25], that can generate cellular oscillations. In a cell cycle oscillator the need for an unambiguous signal for the entry to mitosis may favor a relaxation oscillator. However, these two mechanisms are clearly not mutually exclusive. Mathematically, a typical way in which relaxation (or "hysteresis-driven") oscillators arise is by a coupling of a slow parameter adaptation to the dynamics of a bistable system. We illustrate this mechanism with a simple example. Suppose that a one-dimensional parameterized system $\dot{x} = F(x, z)$ has a bifurcation diagram that looks like the curve shown in Figure 1, where the horizontal axis indicates the parameter z, with solid arrows showing the vector field. In the middle range of the parameter space is a region of bistability where two stable and one unstable equilibria coexist.

Now suppose that the parameter z itself is a function of the state x, $\dot{z} = \epsilon g(x, z)$, $\epsilon \ll 1$, with a "negative feedback" rule that the parameter will slowly increase when x is above the

†Department of Mathematical Sciences, Montana State University, Bozeman, MT 59717 (gedeon@math.montana.edu).
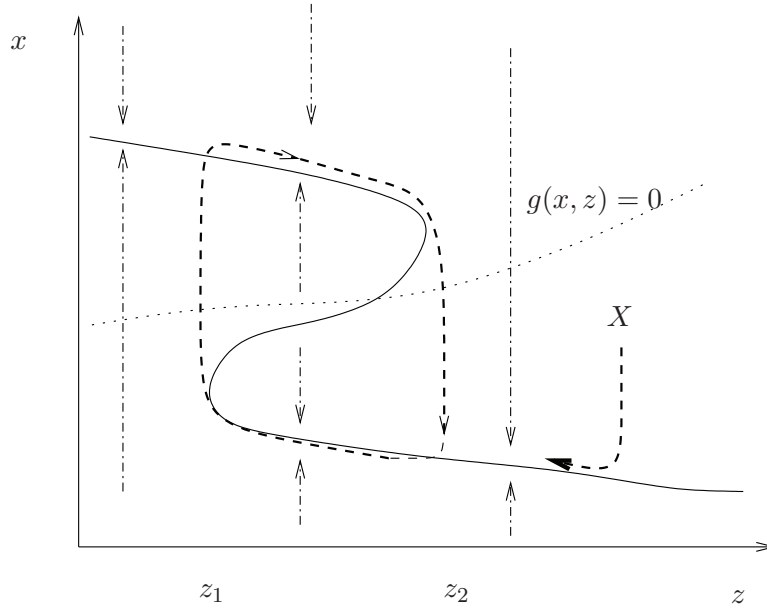
Figure 1. *Relaxation oscillator.*

curve $g(x, z) = 0$ and will slowly decrease when x is below $g(x, z) = 0$. We now analyze what happens when the initial state is at the point labelled "X" in the (z, x) plane. The state x will quickly approach an equilibrium on the lower branch, but as the parameter z slowly decreases, the trajectory in the (z, x) plane will follow the bifurcation curve, until a point at which there are no stable equilibria nearby (the left knee of the bifurcation curve). A fast transition will occur toward the upper branch. Now the state is above the curve $g(x, z) = 0$, so the feedback rule forces the parameter z to increase. There results an oscillation as shown by the dashed curve. For systems where the state variable x is scalar, a rigorous proof that a periodic orbit exists for the joint (z, x) dynamics for sufficiently small ϵ is based on phase-plane techniques in conjunction with the Poincaré–Bendixon theorem and will be presented in Lemma 3.1. This result stems from three essential ingredients: (A) there are two time scales in the problem; (B) the fast dynamics has a cubic-like set of equilibria when viewed as a parameterized family of flows with the slow variable serving the role of the parameter; and (C) the slow dynamics should push the trajectory toward the turning points on the cubic curve of equilibria.

Imagine now that the fast variable x is not scalar but lies in an $\mathbf{R}^n$, while the slow variable z is still scalar. Consider

(1.1)
$$\dot{x} = f(x, z),$$
$$\dot{z} = \epsilon g(x, z).$$

We wish to formulate a set of assumptions analogous to (A), (B), and (C) that would guarantee the existence of a periodic orbit for sufficiently small ϵ in (1.1). We start with an informal discussion and later formulate the assumptions more precisely. The analogue of (B) is an assumption that the set $f(x, z) = 0$ is "cubic-like" with respect to a projection onto the z variable. Note that since $z \in \mathbf{R}$ the set $f(x, z) = 0$ is still a one-dimensional manifold.

Instead of (C) we assume that the hypersurface $g(x, z)$ does not intersect the "upper" and "lower" branches of the cubic, and that the trajectories of the slow flow move toward the knees of the cubic. These assumptions, however, are not sufficient to guarantee the existence of a relaxation periodic orbit for (1.1). The remaining problem is that there is no guarantee that the trajectories of the fast dynamics $\dot{x} = f(x, z)$ in $\mathbf{R}^n$ that starts just off of the knees of the cubic will converge to the equilibrium on the other branch. When x is scalar this is guaranteed by the fact that all solutions of the one-dimensional systems $\dot{x} = F(x, z)$ converge to equilibria, and that the equilibrium on the upper branch is unique for $z < z_1$ and on the lower branch for $z > z_2$.

We show that the convergence result necessary for existence of a relaxation periodic orbit can be recovered if the fast subsystem $\dot{x} = f(x, z)$ of (1.1) is a monotone system. Then the existence of connecting orbits in the neighborhood of both turning points to the other branch follows from the uniqueness of the equilibria past the turning point. In summary, we will show that the existence of a relaxation periodic orbit in (1.1) follows from (A)–(C) when the fast subsystem is monotone.

Our analysis will use input-output characteristics [3, 12, 13, 15]. Because for some range of z the system $\dot{x} = f(x, z)$ will have multiple equilibria, we will need to consider a *multi-valued characteristic* [10, 14]. Recent work [18] has shown that such a characteristic can be used to define a Morse decomposition of a global attractor. A Morse decomposition [9] is a collection of compact isolated invariant sets endowed with a partial order. This partial order carries dynamic information: there are no connecting orbits between Morse sets that do not respect this order. The concept of a Morse decomposition is of great practical importance if a nontrivial Morse decomposition can be found without a detailed knowledge of the invariant set. Then the following two-tiered approach to studying complicated invariant sets is feasible. First we find a nontrivial Morse decomposition whose ordering defines in a broad outline the structure of the global dynamics. In the second step, and perhaps using different methods, we study the internal structure of the individual Morse sets. The paper [18] shows how a multivalued input-output characteristic can be used to define a Morse decomposition and also provides conditions under which some Morse sets consist of a single equilibrium. The results in this paper can be used to show the existence of periodic orbits in Morse sets that do not meet these conditions. Therefore our results are complementary to those in [18].

We apply our theory to a model of cell cycle dynamics in *Xenopus* oocytes. This model, developed by Tyson, Pomerening, and others [31, 32, 29, 37] over the last 15 years, is one of the best developed dynamical models of a subcellular process. One of the most striking features of the cell cycle is the abrupt change that signals entry into the M-phase of the cycle. Several experimental papers [31, 32] suggest that the presence of the positive feedback loops is responsible for this switch-like behavior, and that the negative feedback loop is responsible for generating periodic oscillations. The most natural translation of this verbal model into a mathematical framework is to assume the existence of a slow-fast system, where the fast system, composed of a subsystem consisting of positive feedback loops, is bistable and its equilibria form a hysteretic curve. The negative feedback loop is slow and provide a means of traversing the hysteretic curve in such a way that the entire system exhibits a relaxation periodic orbit. As an application of our theory we examine a hypothesis that the cell cycle oscillation is generated by such a mechanism. A simplified model of Pomerening, Kim, and

Ferrell [32] has the form

(1.2) $$\dot{x} = f(x, \epsilon z), \qquad \dot{z} = g(x, z),$$

where $x \in \mathbf{R}^5$, $z \in \mathbf{R}$, and ϵ is small. The change of variables $\zeta = \epsilon z$ produces

$$\dot{x} = f(x, \zeta), \qquad \dot{\zeta} = \epsilon g\left(x, \frac{\zeta}{\epsilon}\right),$$

which is not a fast-slow system. We will apply our methods to a closely related system where we rewrite the second equation as

$$\dot{\zeta} = \epsilon_1 g\left(x, \frac{\zeta}{\epsilon_2}\right),$$

fix ϵ_2, and let ϵ_1 go to zero. The resulting system

(1.3) $$\dot{x} = f(x, \zeta), \qquad \dot{\zeta} = \epsilon_1 g\left(x, \frac{\zeta}{\epsilon_2}\right)$$

is a fast-slow system of the form (1.1). For a fixed value of ϵ_2, analysis of (1.3) can prove existence of periodic orbits only for sufficiently small ϵ_1. We check numerically if this orbit persists until ϵ_1 reaches the fixed value of ϵ_2, and thus recover a periodic orbit generating the cell cycle in (1.2). The value of ϵ_2 can be interpreted as the strength of the negative feedback in the cell cycle control, and we examine the behavior of this system for a range of values of ϵ_2. We find that if ϵ_2 is too small, the cell cycle is abolished, while if it is too large, the numerical simulation suggests that the periodic orbit disappears before ϵ_1 reaches ϵ_2. There is a bounded interval of feedback strengths ϵ_2 for which we show analytically that (1.3) admits a periodic orbit for small ϵ_1 and show numerically that this orbit persists until $\epsilon_1 = \epsilon_2$. This shows that the cell cycle oscillator requires the negative feedback strength to be in an interval bounded away from zero and infinity.

2. Statement of the main result. We first motivate our approach by a series of informal observations and a simple example. One approach to studying slow-fast systems of the type (1.1) is to analyze first the *fast subsystem*

(2.1) $$\dot{x} = f(x, z), \qquad \dot{z} = 0$$

as a parameterized family of flows. If this system is relatively simple, for each z we can find the set of equilibria. These equilibria form one-dimensional manifolds when z is varied. By changing time $\tau = \epsilon t$ and subsequently setting $\epsilon = 0$ the *slow subsystem*

$$0 = f(x, z), \qquad \dot{z} = g(x, z)$$

describes the slow dynamics along the manifolds of equilibria of the fast subsystem. The analysis of slow-fast systems proceeds by forming concatenations of solutions of the fast subsystem and the slow subsystem and then using either geometrical or topological methods to show that the full system (1.1) has a solution in the neighborhood of this concatenation.

We assume that the function $g(x, z)$ depends only on a subset y of the x variables. Then the dynamics of the slow subsystem depends only on the value of y on the set of equilibria $0 = f(x, z)$. In particular, let h be a function such that $y = h(x)$ and $y \in \mathbf{R}^k$ with $k \ll n$. Then the slow-fast analysis of (1.1) is equivalent to the analysis of the *open loop system* [2, 4]

$$(2.2) \qquad \dot{x} = f(x, z), \qquad y = h(x)$$

in combination with the slow equation

$$\dot{z} = \epsilon g(y, z),$$

where it is understood that y needs to be evaluated only at the equilibria satisfying $0 = f(x, z)$. In the language of control theory, z is the input, x is the state, $h(x)$ is an output function, and y is the output of the open loop system.

Example 1. We introduce a simple illustrative example. Consider

$$(2.3) \qquad \begin{aligned} \dot{w} &= -w + 2y, \\ \dot{y} &= -y(y^2 - 1) + w - z, \\ \dot{z} &= \epsilon(4y - z). \end{aligned}$$

Here the $x = (w, y)$ are fast variables, and $z \in \mathbf{R}$ is the slow variable. Note that the function $g(x, z) = 4y - z$ does not depend on all state variables $x := (w, y)$ but only on the variable y. Therefore the output function h is a projection from the state (w, y) to the second coordinate y. The open loop system consists of the first two equations with z as an input and the output function $y = h(w, y)$.

The concept of an open loop system leads naturally to the concept of an *input-output characteristic*, which we define next. Such a characteristic is usually a function; however, for our purposes we will need a more general notion of a *multivalued input-output characteristic*.

Definition 2.1. *We say that the controlled dynamical system*

$$(2.4) \qquad \dot{x} = f(x, z), \quad y = h(x)$$

is endowed with an input-state characteristic $k_x(u) : Z \to X$, $Z \subset \mathbf{R}$, $X \subset \mathbf{R}^n$, *if for each constant input* $z(t) \equiv \bar{z}$ *there exists a (necessarily unique) globally asymptotically stable equilibrium* $k_x(\bar{z})$ *of system* (2.4). *We also define the* input-output characteristic *as*

$$k(z) := h(k_x(z)), \quad k : Z \to Y, \ Z \subset \mathbf{R}, \ Y \in \mathbf{R}^k.$$

A multivalued input-state characteristic [18] *assigns for each constant input* $z(t) \equiv \bar{z}$ *a finite set of equilibria* $k_x(\bar{z})$ *of system* (2.4) *that attracts a generic set of initial data. The* multivalued input-output characteristic *is the value of the output function h on the set $k_x(z)$:*

$$y := k(z) := h(k_x(z)), \quad k : Z \to Y, \ Z \subset \mathbf{R}, \ Y \in \mathbf{R}^k.$$

In Example 1 the open loop system admits a multivalued input-state characteristic, which consists of the set of equilibria given implicitly by

$$(2.5) \qquad C := \{(x, y, z) \mid z = -y(y^2 - 1) + w, \ w = 2y\}.$$

For each z there are one, two, or three equilibria in C, corresponding to one, two, or three roots of $z = -y(y^2 - 1) + 2y = -y(y^2 - 3)$. Since the output function $y = h(w, y)$ is a projection to the y-coordinate, the input-output characteristic $y = k(z)$ is given implicitly by $z = -y(y^2 - 3)$.

We now focus on the special case of existence of relaxation-type periodic orbits in the fast-slow system (1.1). We assume for simplicity that $k = 1$ and thus $y \in \mathbf{R}$ is scalar. We will take the previous discussion a step further and realize that the existence of the relaxation periodic orbit does not depend on the *dynamics* of the fast system itself, but only on the static shape of the set of equilibria and its relationship with the slow flow nullcline $g(y, z) = 0$. More precisely, only the relative positions of the input-output characteristic $y = k(z)$, which captures the value of y on the set of equilibria, and the nullcline $g(y, z) = 0$ set up the necessary geometry for the existence of a relaxation periodic orbit. From this there is only a small step to realizing the characteristic $y = k(z)$ as a nullcline in a planar system

$$(2.6) \qquad \begin{aligned} \dot{y} &= k^{-1}(y) - z, \\ \dot{z} &= \epsilon g(z, y), \end{aligned}$$

where we replaced the first equation in (1.1) by a scalar equation involving just the output variable y of (2.2). Notice that since $k(z)$ is multivalued, we need to use its inverse which we assume is single-valued. We will use this planar system as a toy system that captures all the essential parts of the system (1.1) needed to establish existence of a relaxation periodic orbit in (1.1).

For Example 1, since $k^{-1}(y) = -y(y^2 - 3)$, we construct the toy system (2.6) as

$$\begin{aligned} \dot{y} &= -y(y^2 - 3) - z, \\ \dot{z} &= \epsilon(4y - z). \end{aligned}$$

A qualitative description of the dynamics of this system is shown in Figure 1.

The remaining two assumptions are the negative feedback $\frac{\partial f}{\partial z} < 0$ and the *monotonicity* of (2.2). The first is used to establish that the multivalued characteristic is weakly nonincreasing [10] in section 3 and therefore has a shape similar to that of Figure 1. The second key ingredient is the *monotonicity* of (2.2); as we noted in the introduction, this is essential to proving that the solutions coming off of the knees of the manifold of equilibria reach the remaining branch of the equilibria.

We now briefly review essentials of the monotone system theory and then proceed to precise formulation of the assumptions that we have just outlined. For more background on monotone systems we refer the reader to [2, 35]. A *cone* is a closed, convex set with nonempty interior and with $\alpha K \subset K$ for $\alpha \in \mathbf{R}^+$ and $K \cap (-K) = \{0\}$. If a space X is endowed with a cone K_x, we will write

$$x \succeq y \text{ iff } x - y \in K_x, \quad x \succ y \text{ iff } x \succeq y, x \neq y, \quad \text{and} \quad x \succ\succ y \text{ iff } x - y \in \text{int } K_x.$$

We say that two points $x, y \in X$ are *order related* if either $x \succ y$ or $y \succ x$ with respect to cone K_x. We assume that the input space Z, the state space X, and the output space Y each has a distinguished cone $K_z \in Z$, $K_x \in X$, and $K_y \in Y$. Since both $Z, Y \subset \mathbf{R}$, the cones K_z and K_y may be either $\mathbf{R}^+$ or $\mathbf{R}^-$, and we assume that both are $\mathbf{R}^+$.

We say that the controlled dynamical system (2.2) is a *monotone system with outputs* if the following two implications hold:

$$z_1(t) \succeq z_2(t) \; \forall t, \; x_1 \succeq x_2 \implies \psi(t, x_1, z_1) \succeq \psi(t, x_2, z_2),$$

$$x_1 \succeq x_2 \implies h(x_1) \succeq h(x_2),$$

where ψ is the flow generated by (2.2) and the $\succeq$ is with respect to appropriate cones. We say that the controlled dynamical system is *strongly monotone* if it is monotone and

$$z_1(t) \succeq z_2(t) \; \forall t \quad \text{and} \quad x_1 \succ x_2 \implies \psi(t, x_1, z_1) \succ\succ \psi(t, x_2, z_2) \; \forall t > 0.$$

Infinitesimal characterizations of monotonicity, which are more suitable for verification, can be found in [2] and [35].

Our assumptions come in three groups. The first set will establish the existence of a cubic-like set of equilibria and is placed on the multivalued characteristic $y = k(z)$. The second set of assumptions are assumptions on the monotonicity and the general structure of the system. Only the last set of assumptions is placed directly on the full system (1.1). With one exception, these assumptions hold for a generic function f, that is, for an f in an open and dense subset of C^2 functions $\mathbf{R}^{n+1} \to \mathbf{R}^n$ in the compact-open topology. Since we are interested in the existence of a stable periodic orbit we impose a nongeneric assumption that the equilibria on the branches analogous to the upper and lower branches in Figure 1 are stable.

Assumption 1. Assume that the characteristic $k(z)$ satisfies the following:
- There are values $0 < z_{min} < z_1 < z_2 < z_{max}$ in Z such that the characteristic $y = k(z)$ is single-valued in $[z_{min}, z_1)$ and $(z_2, z_{max}]$ and multivalued in $[z_1, z_2]$.
- For each $z \in [z_{min}, z_{max}]$ the values $k(z)$ are order-related with respect to the cone K_y.
- Two branches $V_{top} := \max_{z \in [z_{min}, z_2)} \{k(z)\}$ and $V_{bot} := \min_{z \in (z_1, z_{max}]} \{k(z)\}$ satisfy

$$g(z, V_{bot}) < 0 \quad \text{and} \quad g(z, V_{top}) > 0.$$

- The set of values $k(z)$ is connected, and $k^{-1}(z)$ is single-valued.

Assumption 1 implies that $k(z)$ has a shape similar to the cubic-like curve in Figure 1 with some important differences. We assume only that between z_1 and z_2 the system is multistable and thus it may have more than the three equilibria depicted in Figure 1.

It follows from (2.5) that in Example 1 we have $z_1 = -2$, $z_2 = 2$, and for all $z \in (-2, 2)$ there are three equilibria of the form $(2y_1, y_1)$, $(2y_2, y_2)$, $(2y_3, y_3)$, where $y_1 \leq y_2 \leq y_3$ solve $z = -y(y^2 - 3)$. It follows that the equilibria are ordered with respect to the positive orthant. This verifies the first two subassumptions. Since the slow nullcline $z = 4y$ intersects the cubic-like set C (2.5) only at the point $(0, 0, 0)$, the third subassumption follows by inspection. Since $k^{-1}(z) = -y(y^2 - 3)$ the last subassumption holds as well.

Assumption 2. Assume that the following hold:
- For all z the system (2.1) is strongly monotone, $\frac{\partial f}{\partial z} < 0$, and its solutions are bounded.
- We denote by $k_x(z)$ the input-state characteristic of (2.1). We assume that h is injective on the set of equilibria $k_x(z), u \in [z_{min}, z_{max}]$.
- The matrix $dF(x^*, z^*)$ with $F = (f, \epsilon g)^T$ and (x^*, z^*) an equilibrium in $M_{top} := h^{-1}(V_{top})$ or in $M_{bot} := h^{-1}(V_{bot})$ is irreducible.

In Example 1 the off-diagonal entries in the Jacobian of the fast system are positive for any z. This implies that the fast system is cooperative and irreducible and therefore strongly monotone [35]. The rest of the subassumptions are straightforward to verify.

Assumption 3. Assume that for the system (2.1) the following hold:
- There is $\delta > 0$ such that for all $z \in [z_1 - \delta, z_2)$ the upper branch M_{top} consists of stable equilibria and for all $z \in (z_1, z_2 + \delta)$ the lower branch M_{bot} consists of stable equilibria.
- At $z = z_1$ and at $z = z_2$ the set of equilibria $k_x(z)$ undergoes a generic saddle-node bifurcation.
- Homoclinic orbits, if they exist, are isolated.
- Solutions of (2.1) with $z = z_1$ and $z = z_2$ on the unstable manifold of the semistable equilibrium at the limit-point bifurcation converge to the set of equilibria. Recall that by [35, Theorem 4.3] in a strongly monotone system for a generic $x \in \mathbf{R}^n$, $\omega(x)$ is contained in the set of equilibria. Therefore this subassumption is generic in the class of functions satisfying Assumption 1.

In Example 1, the stability analysis reveals that the equilibria corresponding to the upper and lower branches of the cubic $z = -y(y^2 - 3)$ are stable and the middle equilibrium is unstable. This verifies the first subassumption, which is the only nongeneric subassumption in this set.

Theorem 2.2. *Assume Assumptions* 1, 2, *and* 3. *Then the original system* (1.1) *admits a periodic orbit for all sufficiently small* ϵ.

We now outline the proof of the main result. In section 3 using geometrical techniques we show that if the characteristic satisfies Assumption 1, the model system (2.6) admits a positively invariant set in the shape of an annulus. Existence of such a set together with a Poincaré section implies existence of a periodic orbit in $\mathbf{R}^2$. There is a generalization of this result to higher-dimensional spaces, based on the Conley index theory, due to McCord, Mischaikow, and Mrozek [26]. We will use the existence of the positively invariant set in $\mathbf{R}^2$ to construct such a set in $\mathbf{R}^{n+1}$ (the phase space of the full system (1.1)) and verify the assumptions of McCord's result. We first identify a two-dimensional manifold in the neighborhood of the equilibria of the system (2.1) which can be mapped diffeomorphically to a neighborhood of the set of equilibria of the model problem. This map is an extension of the output map h and respects the direction of the flow. We can extend this map to a neighborhood of the connecting orbits from the knee of M_{top} to M_{bot} and from the knee of M_{bot} to M_{top}. The key fact that these connections exist in $\mathbf{R}^n$ uses Assumptions 2 and 3. The inverse image by this map takes the annular neighborhood of the equilibria of the model problem (2.6) to a set, which can be extended to a neighborhood of the equilibria of (2.1). We show that for all ϵ small enough this neighborhood is an isolating neighborhood for system (1.1), and we compute its Conley index. After verifying that the neighborhood admits a Poincaré section, we conclude that there is a periodic orbit in the neighborhood for all sufficiently small ϵ.

3. The model problem. We now consider a planar problem (2.6) and its fast subsystem (4.1). Let $V := \{(y, z) \in \mathbf{R}^2 \mid z = k^{-1}(y)\}$. When we view the curve V as a set of equilibria of (4.1), at $z = z_1$ and $z = z_2$ $(z_1 < z_2)$ this system undergoes limit-point bifurcations. Let (y_1, z_1) and (y_2, z_2) be the corresponding points on V. Since the multivalued characteristic $y = k(z)$ arises from a negative feedback system, it is weakly nonincreasing [10]. It follows that $V_{top} = \{(y, z) \in V \mid y > y_2, z \in [z_{min}, z_2)\}$ and $V_{bot} = \{(y, z) \in V \mid y < y_1, z \in (z_1, z_{max}]\}$.

Since (y_1, z_1) is a limit-point bifurcation point, there is another branch of equilibria, which we denote V_{mid}^1, that joins V_{bot} and terminates at (y_1, z_1). Similarly, in the neighborhood of (y_2, z_2) there is a branch of equilibria V_{mid}^2 that joins V_{top} and terminates at (y_2, z_2). We do not need to assume that V_{mid}^2 is a part of the same branch as V_{mid}^1, even though in our figures we will do so. We need only existence of these branches near the points (y_i, z_i), $i = 1, 2$. In order to ease the notation we will denote both local manifolds V_{mid}^1 and V_{mid}^2 by V_{mid}. We define

$$M_{mid} := h^{-1}(V_{mid}).$$

We denote by $\mathcal{Z}$ a curve in $\mathbf{R}^2$, depicted in Figure 2(a), that consists of $V_{bot} \cup V_{top}$ and the two vertical connecting pieces. Let

$$\mathcal{G} := \{(y, z) \in \mathbf{R}^2 \mid g(z, y) = 0\}.$$

By Assumption 1 the set $\mathcal{G}$ does not intersect $V_{top} \cup V_{bot}$.
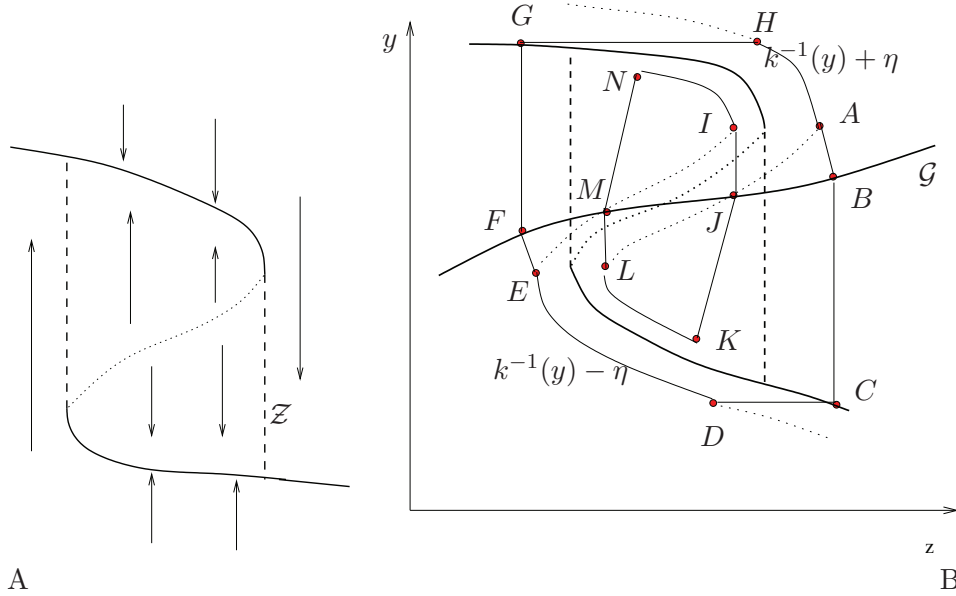
Figure 2. (a) *The $\mathcal{Z}$ curve.* (b) *The set N in the neighborhood of the $\mathcal{Z}$ curve that is positively invariant under the flow of* (2.6).

We now recall a classical construction, which can be found in Lefschetz [24] and Hale [21].

Lemma 3.1. *For any $\delta > 0$ there exist an $\epsilon_0 > 0$ and an open set N, lying within a distance δ of $\mathcal{Z}$, that is positively invariant for* (2.6).

Proof. The construction is seen most easily with the aid of a picture; see Figure 2(b). We construct the boundary of the set N. Draw graphs of $z = k^{-1}(y) \pm \eta$ for some constant η; take a point A on the graph of $z = k^{-1}(y) + \eta$ just above (in y-coordinate) the right turning point (z_2, y_2) of $z = k^{-1}(y) + \eta$. Note that for sufficiently small η the point A is above $\mathcal{G}$; we assume that η has this property. Now we draw a line with negative slope to a point B on the curve $\mathcal{G}$, and then draw a vertical line to a graph $z = k^{-1}(y)$ at point C. This is followed by

a horizontal line to a point D on the graph of $z = k^{-1}(y) - \eta$ and then a piece of the graph of $z = k^{-1}(y) - \eta$ to a point E just below the left turning point (z_1, y_1) of $z = k^{-1}(y) - \eta$. Here we again assume that η is sufficiently small so that E is below the curve $\mathcal{G}$. This point is symmetric to the point A, and we finish the construction in a symmetric way by constructing points F, G, and H. This finishes the outer boundary of N. The inner boundary consists of two pieces of graphs $z = k^{-1}(y) \pm \eta$, two vertical pieces, and two pieces with positive slope (Figure 2(b)).

Now we show that the flow of (2.6) is pointing inward on the outer boundary of N. As a guide we will use the vector field generated by (4.1); if it points inward on the boundary of N, so does the vector field of (2.6) for small ϵ. On the segment AB the slope is negative, and the vector field of (4.1) is vertical and pointing down so it points in on AB. Analogous reasoning applies for segments CD and DE, using the fact that E is below the left turning point of $z = k^{-1}(y) - \eta$. By symmetry, the vector field points in on EF, GH, and HA. The argument for BC and FG cannot be made using (4.1), since these lines are vertical. However, by Assumption 1 the second equation in (2.6) causes the vector field to point left along BC and right along FG, as desired.

Analogous arguments can be used for the inner boundary, and by choosing η sufficiently small, we can make N to be in a δ neighborhood of $\mathcal{Z}$ for any $\delta > 0$. $\blacksquare$

4. Relating (2.1) to the toy problem. In this section we investigate the relationship between dynamics of the parameterized system (2.1) in $\mathbf{R}^n$ and the scalar parameterized system

$$(4.1) \qquad \qquad \dot{y} = k^{-1}(y) - z, \qquad \dot{z} = 0.$$

An immediate observation is that the multivalued input-state characteristic of (4.1) with input z is $y = k(z)$ since we made the output y of (2.6) the state of the system (4.1). Hence the input-state characteristic $x = k_x(z)$ of (2.6) is related to the input state characteristic of $k(z) = h(k_x(z))$ of (4.1) by the output map h. We now analyze the consequences of these observations and Assumption 1 for the fast subsystem (2.1).

Lemma 4.1. *Assume all assumptions of Theorem 2.2.*
1. *The pair (x^*, z^*) is an equilibrium of (1.1) if and only if the pair (y^*, z^*), $y^* = h(x^*)$, is an equilibrium of (2.6).*
2. *The pair (x^*, z^*), for some $x^* \in k_x(z^*)$, is an equilibrium of (2.1) if and only if the pair (y^*, z^*) with $y^* = h(x^*)$ is an equilibrium of (4.1).*
3. *The system (4.1) undergoes a limit-point bifurcation at $z = z^*$ if and only if (2.1) undergoes a limit-point bifurcation at the same value of $z = z^*$.*
4. $M_{bot} \cap M_{top} = \emptyset$.

Proof. 1. The equilibria of (1.1) satisfy $f(x, -z) = 0$, $g(z, y) = 0$, and $y = h(x)$. By the definition of the input-state characteristic k_x, which takes z to a set of equilibria of $\dot{x} = f(x, -z)$, this is equivalent to

$$f(x, -k_x^{-1}(x)) = 0, \quad y = h(x), \quad g(z, y) = 0.$$

Using the first two equations we have

$$z = k_x^{-1}(x) = k_x^{-1}(h^{-1}(y)) = k^{-1}(y).$$

These, together with $g(z, y) = 0$, are the equations for the equilibria of (2.6).

2. The proof follows from the same argument.

3. The proof follows by applying the output function h to the set of equilibria $k_x(z)$ of (1.1). Since h is C^2 and 1-1 on the set of equilibria, it maps the set $k_x(z)$, $z \in [z_{min}, z_{max}]$, diffeomorphically onto the set $k(z)$, $z \in [z_{min}, z_{max}]$.

4. The proof follows from the fact that h is a homeomorphism on the set of equilibria, once we show that $V_{bot} \cap V_{top} = \emptyset$. To show this claim observe that by Assumption 1 there are multiple ordered equilibria for $z \in [z_1, z_2]$. Thus the maximal equilibrium is disjoint from the minimum equilibrium for each $z \in [z_1, z_2]$. Since only V_{top} is defined for $z \in [z_{min}, z_1)$ and V_{bot} is defined for $z \in (z_2, z_{max}]$, the sets V_{bot} and V_{top} are disjoint. ■

The essential step in the description of the correspondence between (4.1) and (2.1) is a definition of special coordinates in the neighborhood of the set of equilibria of (2.1). We start by using the Lyapunov–Schmidt reduction [20] at the limit-point bifurcation (z_1, x_1). Since the limit-point bifurcation at z_1 is generic, by [20, Proposition 9.1] in the neighborhood U_1 of the point (z_1, x_1) there are local coordinates $(z, q_1, q_2) \in \mathbf{R} \times \mathbf{R} \times \mathbf{R}^{n-1}$ in which the flow of (2.1) has the form

$$(4.2) \qquad \dot{q}_1 = (z - z_1) - q_1^2,$$
$$\dot{q}_2 = A_1(z)(q_1, q_2)^T + h_1(z, q_1, q_2),$$

where $h_1(q, z) = O(||q||^2)$ as $||q|| \to 0$. Since we assume that M_{bot} consists of stable equilibria (Assumption 3) all eigenvalues of $A_1(z)$ are negative and bounded away from zero.

Similarly, near (z_2, x_2) there are local coordinates $(z, w_1, w_2) \in \mathbf{R} \times \mathbf{R} \times \mathbf{R}^{n-1}$ in a neighborhood U_2 of (z_2, x_2) in which the flow of (2.1) has the form

$$(4.3) \qquad \dot{w}_1 = (z_2 - z) - w_1^2,$$
$$\dot{w}_2 = A_2(z)(w_1, w_2)^T + h_2(z, w_1, w_2),$$

with h_2 and A_2 having the same properties as h_1 and A_1, respectively. By taking U_1 and U_2 smaller, if necessary, we can assure that $U_i \cap \mathcal{G} = \emptyset$ for $i = 1, 2$. Further, since the bifurcations at z_1 and z_2 are generic, and equilibria on M_{top} and M_{bot} are stable in U_2 and U_1, respectively, we can assume without a loss of generality that all equilibria in $(U_1 \cup U_2) \cap M_{mid}$ have a one-dimensional unstable manifold. Now we prove a global result which uses in an essential way the fact that for each fixed z the system (2.1) is monotone. This result has been proved in [19], but since it is the key to the results of this paper, we reprint it here for completeness.

Lemma 4.2. *Assume all assumptions of Theorem* 2.2. *Take* x *in the branch of the unstable manifold of a point* $w \in M_{mid} \cap U_2$ *that leaves* U_2 *in finite time. Then* $\omega(x) \subset M_{bot}$. *Similarly, for* x *in the branch of the unstable manifold of a point* $w \in M_{mid} \cap U_1$ *that leaves* U_1 *in finite time, we have* $\omega(x) \subset M_{top}$.

Proof. We prove only the first part, since the proof of the second part is analogous. Let

$$\pi : U_2 \times \mathbf{R}^n \to U_2$$

be the coordinate projection. The system (2.1) generates a parameterized flow ψ; that is, for each fixed z, the flow preserves the z-slice of the phase space. We denote the induced flow by ψ^z. Let $(\mu, z_2]$ be the set of all values of z in $\pi(U_2)$ smaller than z_2.

Take arbitrary $z \in (\mu, z_2]$. Then by (4.3) there are two equilibria w^z_{mid} and w^z_{top} in U_2, the second being stable and the first with a one-dimensional unstable manifold. Further, one branch of the unstable manifold of w^z_{mid} connects to w^z_{top}. We denote by Ξ^z the other branch of $W^u(w^z_{mid})$. By Assumption 1 and continuity, for sufficiently small μ there is a single additional equilibrium of ψ^z; it lies on M_{bot}, and we denote it by w^z_{bot}.

We now show that there is an interval $(\nu, z_2] \subset (\mu, z_2]$ such that for all $z \in (\nu, z_2]$ and all $x^z \in \Xi^z$, $\omega(x^z) = w^z_{bot}$.

First, for a generic f (Assumption 3) and all $x^{z_2} \in W^u(w^{z_2}_{mid}) = \Xi^{z_2}$ the omega-limit set $\omega(x^{z_2})$ is contained in the set of equilibria. Further, by assumption the flow ψ^z is strongly monotone. It follows from [35, Theorem 4.3] that for a generic $x \in \mathbf{R}^n$, $\omega(x)$ is contained in the set of equilibria. Therefore there is $\mu_1 < z_2$ such that for all $z \in (\mu_1, z_2]$ and all $x^z \in \Xi^z$, $\omega(x^z)$ is contained in the set of equilibria.

Since the bifurcation at $z = z_2$ is generic (Assumption 3), there are no homoclinic orbits to $w^{z_2}_{mid}$. Further, for a generic f (Assumption 3), the homoclinic orbits are isolated. Therefore there is a μ_2 with $\mu_1 \leq \mu_2 < z_2$ such that for all $z \in (\mu_2, z_2]$ and any $x^z \in \Xi^z$, the omega-limit set $\omega(x^z) \neq w^z_{mid}$.

Finally, since by Assumption 2 all solutions of (2.1) are bounded, for all $z \in (\mu_2, z_2]$ and all $x^z \in \Xi^z$ either $\omega(x^z) = w^z_{top}$ or $\omega(x^z) = w^z_{bot}$. We first note that these conditions are open; that is, if $\omega(x^{z_0}) = w^{z_0}_{bot}$, then for all z with $|z - z_0|$ sufficiently small we have $\omega(x^z) = w^z_{bot}$ for all $x \in \Xi^z$. Therefore either there is a ν with $\mu_2 \leq \nu < z_2$ such that for all $z \in (\nu, z_2]$ and all $x^z \in \Xi^z$ we have $\omega(x^z) = w^z_{bot}$, or there is a sequence $\{\zeta_n\}^\infty_{n=1} \subset (\mu_2, z_2]$ such that $\lim_{n \to \infty} \zeta_n = z_2$ such that for all $x^{\zeta_n} \in \Xi^{\zeta_n}$, $\omega(x^{\zeta_n}) = w^{\zeta_n}_{top}$.

We assume the second case and show that this leads to a contradiction. Observe that in the second case all solutions on both branches of $W^u(w^{\zeta_n}_{mid})$ converge to the point $w^{\zeta_n}_{top}$, and this is true for all n. By continuity and by the fact that the bifurcation at z_2 is generic, there exists a periodic orbit for $z > z_2$, with $z - z_2 \ll 1$; see Figure 3. Since the branch M_{top} consists of stable equilibria, this periodic orbit must be stable for $z > z_2$, with $z - z_2 \ll 1$. This contradicts the fact that the stable periodic orbits do not exist in monotone dynamical systems [35, Theorem 4.3]. Therefore there is an interval $(\nu, z_2]$ such that for all $z \in (\nu, z_2]$ and all $x^z \in \Xi^z$, $\omega(x^z) = w^z_{bot}$. The result now follows if we choose U_2 satisfying $\pi(U_2) \subset (\nu, \infty)$.

A similar argument proves the statement for the neighborhood U_1. $\blacksquare$

Let

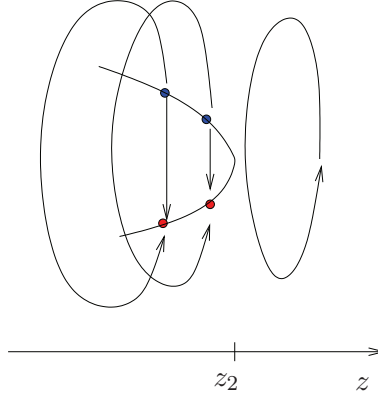$$\mathcal{M} := M_{top} \cup M_{bot} \cup (M_{mid} \cap (U_1 \cup U_2)).$$

We extend the local coordinates defined around the bifurcation points to a neighborhood of $\mathcal{M}$.

Lemma 4.3. *There is a neighborhood U of $\mathcal{M}$ with $U_1 \cup U_2 \subset U$ and coordinates $(z, p, q) \in \mathbf{R} \times \mathbf{R} \times \mathbf{R}^{n-1}$ in U in which the flow (2.1) has the form*

$$\dot{p} = h(z, p),$$
$$\dot{q} = A(z)(p, q)^T + H(z, p, q)$$

such that

1. *in U_1 the coordinates (p, q) agree with the local coordinates (q_1, q_2) defined in (4.2);*

Figure 3. *Limit-point bifurcation gives rise to a stable periodic orbit.*

2. *in U_2 the coordinates (p, q) agree with the local coordinates (w_1, w_2) defined in* (4.3);
3. $H(z, p, q) = O(||(p, q)||^2)$ *as* $||(p, q)|| \to 0$;
4. *all eigenvalues of $A(z)$ are negative and bounded away from zero.*

Proof. We outline the proof; for details see [19]. The main task is to extend the coordinates $(w_1, w_2) \in U_2$ to a neighborhood of M_{bot} and the local coordinates q_1, q_2 from U_2 to a neighborhood of M_{top}.

We first note that if A_w is a linearization of (2.1) at $w = M_{bot} \cap \pi^{-1}(\lambda)$, then the map $x \to A_w x$ is monotone with respect to K_X [3, Lemma 6.4] and the matrix A_w admits a Perron–Frobenius eigenpair (μ_w, e_w). Since the equilibrium w is stable, the eigenvalue $\mu_w \leq 0$. Since by Assumption 2 matrices A_w are irreducible, by Corollary 3.2 of [35] the real part of the rest of the spectrum is strictly smaller than μ_w. Since the spectrum of $A(z)$ contains all eigenvalues of A_w except μ_w, the last statement follows. We use a result of Brunovský [7] to select a one-dimensional stable manifold that is tangent to the eigenvector e_w, which changes continuously with the base point w. The technical difficulties are related to the fact that such a manifold is not necessarily unique and some care has to be applied to its construction; see [19]. ∎

Definition 4.4. *Using the coordinates of Lemma 4.3, we define a two-dimensional manifold in the neighborhood U of $\mathcal{M}$ (see Figure 4):*

$$\mathcal{U} := \{(z, p, q) \in U \mid q = 0\}.$$

Having defined local coordinates in the neighborhood U of $\mathcal{M}$, we relate them to local coordinates in the neighborhood of V via the map h. Recall that ψ denotes the parameterized flow of (2.1), and let φ denote the parameterized flow of (4.1).

Define a mapping $F : \mathcal{U} \to \mathbf{R}^2$ in two stages. First, since (4.1) undergoes a generic limit-point bifurcation at $z = z_1$ and the parameterization of M is continuous, the map h induces a diffeomorphism F taking M to V in such a way that M_{top}, M_{bot}, and M_{mid} map to V_{top}, V_{bot}, and V_{mid}. Take an arbitrary $w_{top}^{z_0} \in M_{top}$. Let B be a neighborhood of z_0 in (z_{min}, z_{max}), and let $\mathcal{U}_B := \{(z, p, q) \in U \mid z \in B, q = 0\}$ be a two-dimensional manifold that is foliated by one-dimensional stable submanifolds $W^s(w_{top}^z)$, $z \in B$. There is also a neighborhood $\bar{\mathcal{U}} \in \mathbf{R}^2$ of $F(w_{top}^{z_0})$ that is foliated by the stable manifolds of points $F(w_{top}^z)$, $z \in B$. We extend F
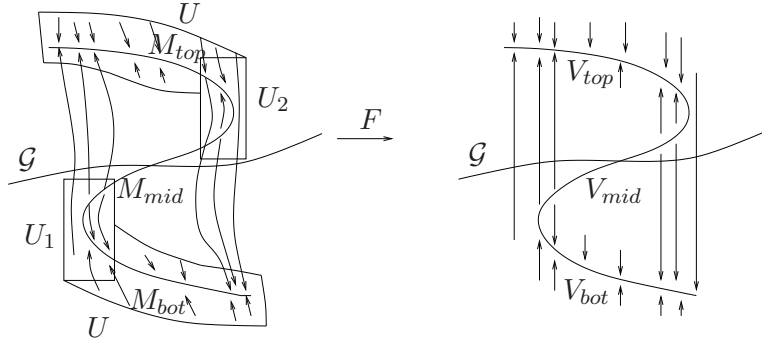
Figure 4. *Map F maps the two-dimensional manifold in the neighborhood of the set M to its image in $\mathbf{R}^2$. The flow ψ (left), generated by (2.1), is orbit equivalent to the flow φ (right), generated by (4.1). The neighborhoods U_1 and U_2 of the turning points on M are also indicated.*

to $\mathcal{U}_B$ in such a way that it maps flow lines of ψ on $\mathcal{U}_B$ to flow lines of φ on $\bar{\mathcal{U}}$ and preserves the direction of the flow. By a similar argument we can define the map F on a neighborhood $\mathcal{U}_B$ of an arbitrary point $w_{bot}^{z_0}$.

Since both systems undergo generic limit-point bifurcations, the map F can be defined in the union $U_1 \cup U_2$.

Definition 4.5 (see [23]). *Two C^r flows, φ on M and ψ on N, are C^m orbit equivalent $(m \leq r)$ if there is a C^m diffeomorphism $h : M \to N$ such that $\chi(t) = h \circ \psi(t) \circ h^{-1}$ is a time reparameterization of the flow φ.*

We summarize our previous construction in the following lemma.

Lemma 4.6. *The flow ψ restricted to $\mathcal{U}$ is orbit equivalent to the flow φ in the neighborhood of $V := F(\mathcal{U})$, via the map F.*

Note that the set V does not contain a full neighborhood of the curve Z from Figure 2(a). We now extend the map F so that it is defined on neighborhoods of trajectories starting at the knees of $\mathcal{M}$ and connecting to the other branches of $\mathcal{M}$. By Lemma 4.2 the omega-limit set of $x \in \mathcal{U} \cap U_1$ lies in M_{top}, and the omega-limit set of $x \in \mathcal{U} \cap U_2$ lies in M_{bot}. In a straightforward way the flows ψ and φ can be used to extend the map F to the set

$$\bigcup_{x \in U_2 \cup U_1} \bigcup_{t \geq 0} \psi(t, x).$$

We call the resulting map, defined on

$$\mathcal{H} := \mathcal{U} \cup \bigcup_{x \in U_2 \cup U_1} \bigcup_{t \geq 0} \psi(t, x),$$

again F. Observe that $F(\mathcal{H})$ contains a neighborhood of the curve $\mathcal{Z}$ in Figure 2.

4.1. Lifting of the planar problem. Let ψ_ϵ denote the flow of (1.1), and let φ_ϵ denote the flow of (2.6).

A set $\mathcal{N}$ is an *isolating neighborhood* if $\operatorname{Inv} \mathcal{N} \subset \operatorname{int} \mathcal{N}$, that is, if the maximal invariant set S in N lies in the interior of $\mathcal{N}$.

An isolating neighborhood N is an *isolating block* if $\partial N = N^+ \cup N^-$, where N^- is the *immediate exit set*

$$N^- := \{x \in N \mid \varphi([0,t],x) \not\subset N \ \forall t > 0\},$$

N^+ is the *immediate entrance set*

$$N^+ := \{x \in N \mid \varphi([t,0],x) \not\subset N \ \forall t < 0\},$$

and both N^+ and N^- are subsets of local sections of the flow.

Lemma 4.7. *Let $N' := F^{-1}(N) \subset \mathcal{H}$, where $N \subset \mathbf{R}^2$ is the neighborhood of the Z-curve constructed in Lemma* 3.1.

Then there are a neighborhood $\mathcal{N}$ of N' in $\mathbf{R}^{n+1}$ and ϵ_0, such that $\mathcal{N}$ is positively invariant under ψ_ϵ for all $\epsilon < \epsilon_0$ and ϵ_0 sufficiently small. In particular, $\mathcal{N}$ is an isolating block under ψ_ϵ.

Proof. We will extend the set $N' \subset \mathcal{H}$ to its neighborhood $\mathcal{N} \in \mathbf{R}^{n+1}$, i.e., a set with a nonempty interior, in such a way that the flow ψ_ϵ on the boundary is transversal inward. This will imply that $\mathcal{N}$ is an isolating block.

There are two main ingredients to the construction. The first is to construct a neighborhood of M_{top} and M_{bot}; the second is the construction of the neighborhood along the connections between the knee of M_{top} and M_{bot} and the knee of M_{bot} and M_{top}. To do the first part we use the local coordinates in U_1 of Lemma 4.3. Since the matrix A_1 has spectrum bounded away from zero, there are $\eta > 0$ and

$$K_1 := \{(q_1, q_2) \in U_1 \mid q_1 \in N' \cap U_1, \ |q_2| \leq \eta_1\},$$

such that ψ_ϵ points inward on the part of the boundary ∂K_1 given by

$$\{(q_1, q_2) \in U_1 \mid q_1 \in N' \cap U_1, \ |q_2| = \eta_1\}.$$

Now we need to check the other parts of the boundary. Lemma 4.6 and continuity imply that for sufficiently small η the flow ψ_ϵ for small ϵ points inward on $\partial K_1 \cap F^{-1}(FE)$; see Figure 2. Since $\dot{z} < 0$ on $\partial K_1 \cap F^{-1}(ML)$, the flow ψ_ϵ points inward on $\partial K_1 \cap F^{-1}(ML)$.

Since $W^u(M_{mid}) \cap \partial K_1 \neq \emptyset$, there is a neighborhood B_1 of $W^u(M_{mid}) \cap \partial K_1$ such that the vector field of (1.1) points outward in B_1. Finally, we extend K_1 along M_{bot} to

$$\bar{K}_1 := \{(q_1, q_2) \in U \mid q_1 \in N', \ |q_2| \leq \eta_1'\},$$

which coincides with K_1 in U_1. Since by Lemma 4.3 $A(z)$ has negative eigenvalues bounded away from zero, we can choose η_1' small enough so that ψ_ϵ points inward on $\partial(K_1 \cup K_1')$ except for the set $B_1 \subset \partial K_1$.

A similar construction can be done in the neighborhood U_2 of the other bifurcation point to construct K_2 and then extend K_2 to a neighborhood $\bar{K}_2$ of $M_{top} \cap N'$. Then flow ψ_ϵ points inward along the boundary $\partial(K_2 \cup K_2')$, except for a neighborhood $B_2 \subset \partial K_2$ of $W^u(M_{mid}) \cap \partial K_2$. This finishes the first step of the construction.

The second step in the construction of the set $\mathcal{N}$ is to extend N' along the preimages by F of the vertical connections from the turning points to the other branch of V.

Take the set $B_1 \subset K_1$ and flow it forward by the flow ψ. By choosing η smaller, if necessary, we can assure that $\psi(x, t(x)) \in \text{int } \bar{K}_2$ for all $x \in B_1$ and some $t(x)$, which depends on x. The

flow ψ between B_1 and the arrival in $\bar{K}_2$ is a parallelizable flow. Take $\bar{B}_1$ a neighborhood of the set B_1 and set

$$\bar{X}_1 := \bigcup_{x \in \bar{B}_1, \, t \in [0, t(x)]} \psi(t, x), \qquad X_1 := \bigcup_{x \in B_1, \, t \in [0, t(x)]} \psi(t, x).$$

We shave the set $\bar{X}_1$ in the way indicated in Figure 5 (right) in such a way that the flow ψ points inward along its boundary. The same property then holds for ψ_ϵ for small ϵ.
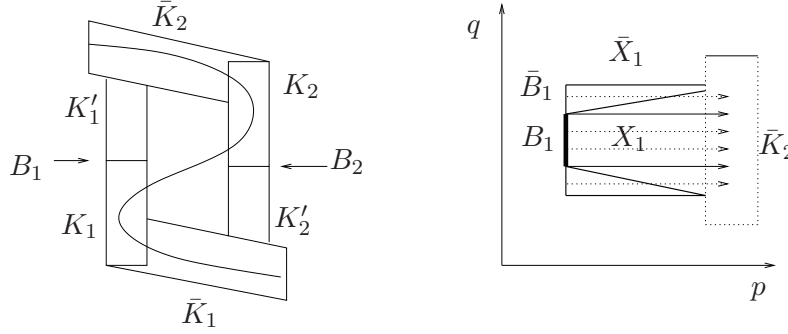
Figure 5. *Left: A projection of various sets into a two-dimensional manifold $\bar{\mathcal{U}}$. Right: Shaving between flow boxes X_1 and $\bar{X}_1$. The picture on the right is in complementary directions to the picture on the left.*

We call this set K_1' and construct an analogous set K_2' by flowing the exit set B_2 of K_2 until it enters $\bar{K}_1$. Let

$$\mathcal{N} := K_1 \cup K_1' \cup \bar{K}_1 \cup K_2 \cup K_2' \cup \bar{K}_2.$$

By construction the flow ψ_ϵ points inward along the boundary $\partial \mathcal{N}$. ∎

5. The Conley index theory. We recall basic definitions of the Conley index theory [9]. Recall that a set $\mathcal{N}$ is an isolating neighborhood if $\mathrm{Inv}\,\mathcal{N} \subset \mathrm{int}\,\mathcal{N}$, that is, if the maximal invariant set S in N lies in the interior of $\mathcal{N}$. Such a set S is an *isolated invariant set*.

The pair of compact sets $L \subset N$ is an *index pair* for an isolated invariant set S if
1. $S = \mathrm{Inv}(cl(N \setminus L))$ and $N \setminus L$ is a neighborhood of S;
2. L is positively invariant in N, i.e., if $x \in L$ and $\varphi([0,t], x) \subset N$, then $\varphi([0,t], x) \subset L$;
3. L is an exit set for N; i.e., given N and $T > 0$ such that $\varphi(T, x) \notin N$, there is $t \in [0, T]$ such that $\varphi([0,t], x) \subset N$ and $\varphi(t, x) \in L$.

Observe that if N is an *isolating block*, then (N, N^-) is an index pair.

The cohomological Conley index $CH(\mathcal{N})$ of an isolating neighborhood $\mathcal{N}$ is defined as a cohomology

$$CH(\mathcal{N}) := H^*(N, L).$$

It can be shown [9] that the index is independent of the choice of the index pair and the choice of the isolating neighborhood. In fact, it depends only on the maximal invariant set $S := \mathrm{Inv}\,\mathcal{N}$, and thus we use the notation $CH(S)$ and talk about the Conley index of an isolated invariant set S.

Given the isolating neighborhood $\mathcal{N}$ and the flow φ, we say that Σ is a Poincaré section for φ in $\mathcal{N}$ if $\Sigma \cap N$ is closed and for every $x \in N$

$$\varphi(x, (0, \infty)) \cap \Sigma \neq \emptyset.$$

Now we are ready to recall a theorem relating the Conley index of $\mathcal{N}$ to the existence of a periodic orbit in $\mathcal{N}$.

Theorem 5.1 (see [26, Theorem 1.3]). *Assume that X is an absolute neighborhood retract and $\Psi : X \times [0, \infty) \to X$ is a semiflow with compact attraction. If N is an isolating neighborhood for ψ which admits a Poincaré section Σ and either*

$$\dim CH^{2n}(N, \Psi) = \dim CH^{2n+1}(N, \Psi) \quad \text{for } n \in Z$$

or

$$\dim CH^{2n}(N, \Psi) = \dim CH^{2n-1}(N, \Psi) \quad \text{for } n \in Z,$$

where not all the above dimensions are zero, then Ψ has a periodic trajectory in N.

6. Proof of Theorem 2.2. We apply Theorem 5.1 to the neighborhood $\mathcal{N} \in \mathbf{R}^{n+1}$ and the flow ψ_ϵ for a sufficiently small ϵ. First we observe that $\mathbf{R}^{n+1}$ is an absolute neighborhood retract and all flows ψ_ϵ are trivially semiflows with compact attraction.

Next we verify that $\mathcal{N}$ admits a Poincaré section. We start with the set B_1 defined in Lemma 4.7. All trajectories starting at B_1 must enter the set $\bar{K}_2$ in finite time. Since $\dot{u} > 0$ in $\bar{K}_2$ and the flow on the boundary of $\mathcal{N}$ points inward, these solutions have to enter K_2 in finite time. In K_2 we still have $\dot{u} > 0$, so there is no invariant set in K_2. Since B_2 is the exit set of K_2, all the trajectories entering K_2 have to leave through B_2 in finite time. Therefore all trajectories starting at B_1 arrive at B_2 in finite time. A symmetric argument starting at B_2 finishes the proof that B_1 is a Poincaré section of $\mathcal{N}$.

We can make a cohomology calculation for the flow (2.6). Since N is an annulus in the plane,

$$H^*(N) = \begin{cases} Z & \text{for } * = 0, 1, \\ 0 & \text{otherwise.} \end{cases}$$

Now we compute the Conley index of $\mathcal{N}$. By Lemma 4.7 $\mathcal{N}$ is an isolating block, and the flow on the boundary is inward. It follows that $(\mathcal{N}, \emptyset)$ is an index pair. Therefore

$$CH^*(\mathcal{N}) = H^*(\mathcal{N}, \emptyset).$$

By construction of $\mathcal{N}$ this set is a topological product of the set N' and a small $(n-1)$-dimensional disc D^{n-1} in the q-directions (Lemma 4.3). Therefore

$$H^*(\mathcal{N}, \emptyset) = H^*(\mathcal{N}) = H^*(N' \times D^{n-1}) = H^*(N') = H^*(F^{-1}(N)).$$

Finally, since F is a homeomorphism, we have

$$H^*(F^{-1}(N)) = H^*(N).$$

Therefore $CH^*(\mathcal{N}) = H^*(N)$, and the Conley index satisfies the assumptions of Theorem 5.1. Therefore $\mathcal{N}$ contains a periodic orbit for all sufficiently small ϵ. ∎

7. Cell cycle model in *Xenopus*. Over the last 15 years great strides have been made toward understanding of a cell cycle oscillator both experimentally [30] and using mathematical models [31, 32, 29, 37]. Several experimental papers [31, 32] suggest that the abrupt change
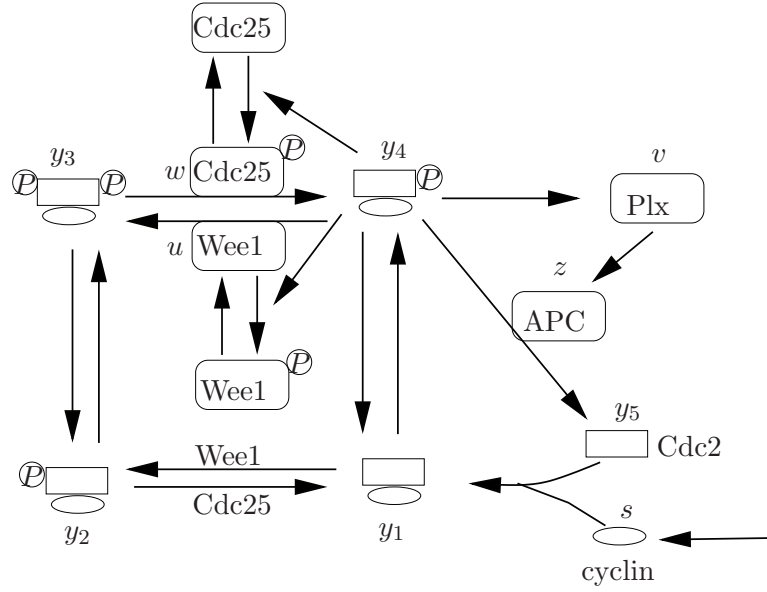
Figure 6. *Schematic description of the cell cycle engine with names of model variables indicated. Cdc2 (rectangle) and cyclin (oval) form a heterodimer, which can be phosphorylated on two distinct residues, Tyr15 and T161. Phosphorylation on the Tyr15 residue is catalyzed by the dephosphorylated form of a kinase Wee1, while the opposing phosphatase is the phosphorylated form of Cdc25. The active Cdc2-cyclin dimer (y_4) is phosphorylated on Thr161, but not on Tyr15. It phosphorylates both Cdc25 and Wee1, activating Cdc25 and deactivating Wee1. In addition, the active form of Cdc2-cyclin activates ubiquitin ligase APC through an intermediary Plx. APC degrades cyclin, which causes destruction of all forms of Cdc2-cyclin dimers. For the sake of clarity, we show the full regulation of Cdc25 and Wee1 only on the top part of the phosphorylation square and destruction of Cdc2-cyclin dimer in only one of its forms.*

that signals entry into the M-phase of the cycle is caused by the bistability generated by the positive feedback loops, while the negative feedback loop supplies the recovery feedback necessary for a periodic oscillation. A model incorporating these ingredients was proposed and numerically analyzed by Novak and Tyson [29] and used later by Pomerening and others (see [31, 32]). Tyson and his collaborators [29, 37] developed a series of models that correlate the observed progression through the checkpoints along the cell cycle to the bifurcation diagrams of the dynamics. Bifurcation diagrams capture the essential dynamics but do not provide a rigorous connection between the periodic orbit and the bistable set of equilibria. The approach developed in this paper links the cell cycle oscillation directly to the relaxation oscillation on a bistable curve of equilibria.

We now review basic biological building blocks that underlie the control of the cell cycle [37] in *Xenopus* embryos; see Figure 6. The central player is a heterodimer Cdc2-cyclin, whose activity is regulated by a synthesis and degradation of cyclin and by a phosphorylation and dephosphorylation of Cdc2.

The activity of Cdc2-cyclin is regulated by three phosphorylation sites: activation site Thr161 and two inhibitory phosphorylation sites Thr14 and Tyr15. Since the latter sites are always dephosphorylated simultaneously, it is sufficient to track the state of Tyr15. In *Xenopus* Thr161 is phosphorylated by CAK and dephosphorylated by PP2c; the kinase that

phosphorylates Tyr15 is Wee1, and the corresponding phosphatase is Cdc25. The active form of Cdc2-cyclin is phosphorylated on Thr161 but not on Tyr15. The rapid onset of the M-phase transition is brought on by rapid conversion of the doubly phosphorylated Cdc2-cyclin to its Thr161 phosphorylated active form. There are two positive feedback loops: Cdc2-cyclin upregulates activity of the phosphatase Cdc25 and downregulates activity of the kinase Wee1. Since phosphatase Cdc25 promotes the active form of Cdc2-cyclin, and the kinase promotes the inactive form of Cdc2-cyclin, both of these constitute positive feedback loops. Cdc2-cyclin dimers are broken up by cyclin degradation, which is promoted by ubiquitin ligase APC. Since Cdc2-cyclin activates APC, this forms a negative feedback loop. Since APC action is significantly delayed, it is very likely that the activation of the APC is accomplished through an intermediary.

7.1. Model development. Our model is based on the model of Pomerening, Kim, and Ferrell [32], which has 13 variables. Three of these variables describe a Cdc2-cyclin complex that cannot be phosphorylated at the T161 position. These represent particular mutants used in the experiments in [32]. The remaining variables represent concentrations of cyclin $(= s)$, a Cdc2-cyclin weakly active [1] nonphosphorylated complex $(= y_1)$, an inactive Tyr15-phosphorylated Cdc2-cyclin complex $(= y_2)$, an inactive Tyr15- and T161-phosphorylated Cdc2-cyclin complex $(= y_3)$, and, finally, an active T161-phosphorylated complex $(= y_4)$. Further, the model tracks the concentration of Cdc2 $(= y_5)$, the active form of Cdc25 $(= w)$, Wee1 $(= u)$, Plx $(= v)$, and APC $(= z)$. The Plx is the putative intermediary in the negative APC-mediated feedback loop. The system of equations takes the form

(7.1)
$$\dot{s} = k_{synth} - k_{dest}sz - k_a y_5 s + k_d y_1,$$

$$\dot{y}_1 = k_a y_5 s - k_d y_1 - k_{dest} y_1 z - k_{wee1} u y_1 - k_{wee1basal}(wee1_{tot} - u)y_1 + k_{cdc25} w y_2$$
$$\quad + k_{cdc25basal}(cdc25_{tot} - w)y_1,$$

$$\dot{y}_2 = k_{wee1} u y_1 + k_{wee1basal}(wee1_{tot} - u)y_1 - k_{cdc25} w y_2 - k_{cdc25basal}(cdc25_{tot} - w)y_2 - k_{cak} y_2$$
$$\quad + k_{pp2c} y_3 - k_{dest} y_2 z,$$

$$\dot{y}_3 = k_{cak} y_2 - k_{pp2c} y_3 - k_{cdc25} w y_3 - k_{cdc25basal}(cdc25_{tot} - w)y_3 + k_{wee1} u y_4$$
$$\quad + k_{wee1basal}(wee1_{tot} - u)y_4 - k_{dest} y_3 z,$$

$$\dot{y}_4 = k_{cdc25} w y_3 + k_{cdc25basal}(cdc25_{tot} - w)y_3 - k_{wee1} u y_4 - k_{wee1basal}(wee1_{tot} - u)y_4 - k_{dest} y_4 z,$$

$$\dot{y}_5 = k_{dest} z(y_1 + y_2 + y_3 + y_4) + k_d y_1 - k_a y_5 s,$$

$$\dot{w} = k_{cdc25on} \frac{y_4^4}{e_{cdc25}^4 + y_4^4}(cdc25_{tot} - w) - k_{cdc25off} w,$$

$$\dot{u} = -k_{wee1off} \frac{y_4^4}{e_{wee1}^4 + y_4^4}u + k_{wee1on}(wee1_{tot} - u),$$

$$\dot{v} = k_{plxon} \frac{y_4^3}{e_{plx}^3 + y_4^3}(plx_{tot} - v) - k_{plxoff} v,$$

$$\dot{z} = k_{apcon} \frac{v^3}{e_{apc}^3 + v^3}(apc_{tot} - z) - k_{apcoff} z.$$

The constants and their values (below) were taken from a supplement of the paper of Pomerening, Kim, and Ferrell [32]). Since the period of the resulting oscillation after removal of the three equations representing species that do not occur in the wild type was $T = 200$, we rescaled the time in such a way that the period changed to the experimentally observed value $T = 80$. Equivalently, this can be achieved by appropriately rescaling all rate constants below by 200/80:

|			
$k_{synth} = 0.4$	cyclin synthesis rate	$k_{dest} = 0.006$	cyclin destruction rate
$k_{wee1} = 0.05$	active Wee1 phosphorylation rate	$k_{wee1basal} = 0.05/15$	basal Wee1 phosphorylation rate
$k_{cdc25} = 0.1$	active Cdc25 dephosphorylation rate	$k_{cdc25basal} = 0.1/15$	basal Cdc25 dephosphorylation rate
$k_{cdc25on} = 1.75$	Cdc25 activation rate	$k_{cdc25off} = 0.2$	Cdc25 deactivation rate
$k_{wee1on} = 0.2$	Wee1 activation rate	$k_{wee1off} = 1.75$	Wee1 deactivation rate
$k_{plxon} = 1$	Plx activation rate	$k_{plxoff} = 0.15$	Plx deactivation rate
$k_{apcon} = 1$	APC activation rate	$k_{apcoff} = 0.15$	APC deactivation rate
$wee1_{tot} = 15$	total Wee1 concentration	$cdc25_{tot} = 15$	total Cdc25 concentration
$plx_{tot} = 50$	total Plx concentration	$apc_{tot} = 50$	total APC concentration
$e_{cdc25} = 40$	Cdc25 half-activation	$e_{wee1} = 40$	Wee1 half-activation
$e_{apc} = 40$	APC half-activation	$e_{plx} = 40$	Plx half-activation

The initial data are $s = 0$, $y_1 = y_2 = y_3 = y_4 = y_6 = y_7 = y_8 = w = u = v = 0$ and $y_5 = 230$, $z = 15$. We will simplify the model in three steps.

1. Since according to [1, 27] (see also [16]) the nonphosphorylated Cdc2-cyclin complex y_1 is weakly active, we try to simplify the equations by lumping together the inactive Tyr15 phosphorylated forms y_2 and y_3 and active Tyr15 nonphosphorylated forms y_1 and y_4. We will replace them by new variables

$$y := y_2 + y_3 \quad \text{and} \quad \eta := y_1 + y_4.$$

Here η represents the active Cdc2-cyclin complexes, and y represents the inactive Cdc2-cyclin complexes. Observe that this is not a simple change of variables because the weak activity of y_1 is not reflected in the system (7.1) and therefore we must replace y_4 in the last four equations and y_1 in the first equation by $\eta = y_1 + y_4$:

$$\dot{s} = k_{synth} - k_{dest}sz - k_a y_5 s + k_d \eta,$$
$$\dot{\eta} = k_a y_5 s - k_d \eta - k_{dest}\eta z - k_{wee1}u\eta - k_{wee1basal}(wee1_{tot} - u)\eta + k_{cdc25}wy$$
$$\quad + k_{cdc25basal}(cdc25_{tot} - w)y,$$
$$\dot{y} = k_{wee1}u\eta + k_{wee1basal}(wee1_{tot} - u)\eta - k_{cdc25}wy - k_{cdc25basal}(cdc25_{tot} - w)y - k_{dest}yz,$$
$$\dot{y}_5 = k_{dest}z(y + \eta) + k_d \eta - k_a y_5 s,$$
$$\dot{w} = k_{cdc25on}\frac{\eta^4}{e_{cdc25}^4 + \eta^4}(cdc25_{tot} - w) - k_{cdc25off}w,$$
$$\dot{u} = -k_{wee1off}\frac{\eta^4}{e_{wee1}^4 + \eta^4}u + k_{wee1on}(wee1_{tot} - u),$$
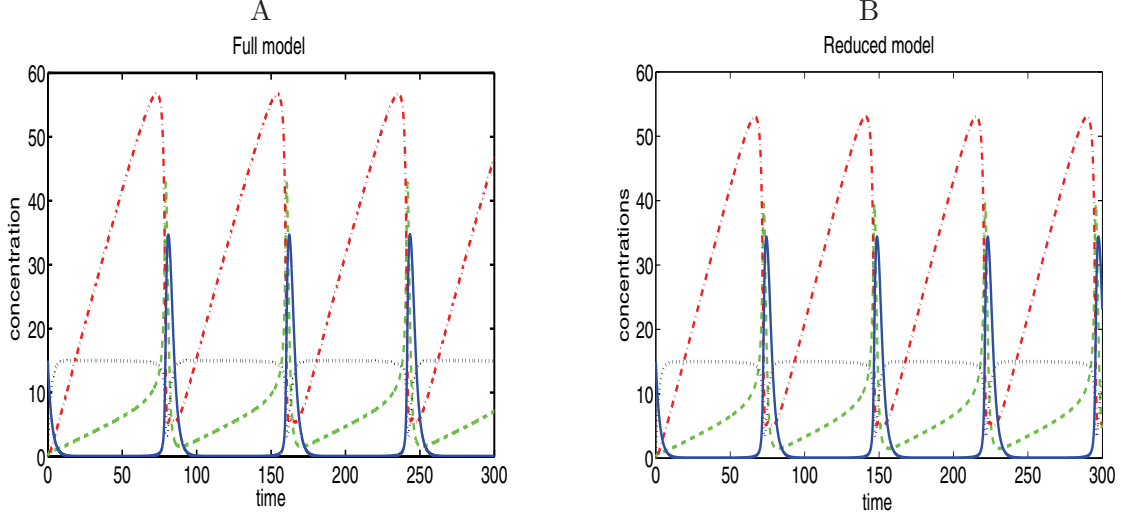
Figure 7. *Comparison of the dynamics of the full model* (7.1) *in* (a) *and the reduced model* (7.2) *in* (b). *In order to compare the appropriate variables we graph in* (a) $y_1 + y_4$ *(dashed green),* $y_2 + y_3$ *(dotted black),* u *(red dash-dot), and* z *(solid blue), and in the reduced model we graph* q *(dashed green),* $x - q$ *(dotted black),* u *(red dash-dot), and* z *(solid blue).*

$$\dot{v} = k_{plxon} \frac{\eta^3}{e_{plx}^3 + \eta^3}(plx_{tot} - v) - k_{plxoff} v,$$

$$\dot{z} = k_{apcon} \frac{v^3}{e_{apc}^3 + v^3}(apc_{tot} - z) - k_{apcoff} z.$$

2. In the second step we add the first two equations and set $q := s + \eta$. We replace each occurrence of η in the resulting sum by the new variable q. Since this addition removes the only dependence on y_5 in all equations except the y_5 equation, we can drop the y_5 equation. These changes imply that we will not track separately free cyclin (s), free Cdc2 (y_5), and their active complex Cdc2-cyclin (represented by η); rather we assume that the active Cdc2-cyclin complex is synthesized directly with the rate k_{synth}. This is consistent with the observation that the free Cdc2 is constitutively expressed in excess of the available cyclin [8]. We note that most of the experimental and modeling papers graph cyclin levels against active Cdc2-cyclin levels to illustrate the hysteresis in the system. Therefore most of the discussion of the role of bistability in the literature is illustrated on this particular two-dimensional projection of the set of equilibria. The theoretical work in the first part of this paper suggests that the proper projection should involve the negative feedback variable and the output variable of the monotone system. The fact that combining cyclin and active Cdc2 variables does not change the dynamics of the system (Figure 7) underscores the conclusion that the phosphorylation of the Cdc2-cyclin complex is the central part of the cell cycle engine. With this change of variables, the equations become

$$\dot{q} = k_{synth} - k_{dest}qz - k_{wee1}uq - k_{wee1basal}(wee1_{tot} - u)q + k_{cdc25}wy$$
$$\quad + k_{cdc25basal}(cdc25_{tot} - w)y,$$
$$\dot{y} = k_{wee1}uq + k_{wee1basal}(wee1_{tot} - u)q - k_{cdc25}wy - k_{cdc25basal}(cdc25_{tot} - w)y - k_{dest}yz,$$

$$\dot{w} = k_{cdc25on} \frac{q^4}{e_{cdc25}^4 + q^4}(cdc25_{tot} - w) - k_{cdc25off}w,$$

$$\dot{u} = -k_{wee1off} \frac{q^4}{e_{wee1}^4 + q^4}u + k_{wee1on}(wee1_{tot} - u),$$

$$\dot{v} = k_{plxon} \frac{q^3}{e_{plx}^3 + q^3}(plx_{tot} - v) - k_{plxoff}v,$$

$$\dot{z} = k_{apcon} \frac{v^3}{e_{apc}^3 + v^3}(apc_{tot} - z) - k_{apcoff}z.$$

3. Our final simplification is a simple change of variables: instead of tracking q (active Cdc2-cyclin) and y (inactive Cdc2-cyclin), we will track the total Cdc2-cyclin $x := y + q$ and the active compound q. This transformation considerably simplifies the second equation. The final system is

$$\dot{q} = k_{synth} - k_{dest}qz - k_{wee1}uq - k_{wee1basal}(wee1_{tot} - u)q + k_{cdc25}w(x - q)$$
$$+ k_{cdc25basal}(cdc25_{tot} - w)(x - q),$$

$$\dot{x} = k_{synth} - k_{dest}xz,$$

(7.2) $$\quad \dot{w} = k_{cdc25on} \frac{q^4}{e_{cdc25}^4 + q^4}(cdc25_{tot} - w) - k_{cdc25off}w,$$

$$\dot{u} = -k_{wee1off} \frac{q^4}{e_{wee1}^4 + q^4}u + k_{wee1on}(wee1_{tot} - u),$$

$$\dot{v} = k_{plxon} \frac{q^3}{e_{plx}^3 + q^3}(plx_{tot} - v) - k_{plxoff}v,$$

$$\dot{z} = k_{apcon} \frac{v^3}{e_{apc}^3 + v^3}(apc_{tot} - z) - k_{apcoff}z.$$

We compare the dynamics of the full model (7.1) and the reduced model (7.2) in Figure 7. Note that the only visible change is a slightly shorter period of the oscillation in the reduced model.

7.2. Input-output characteristic. The system (7.2) is amenable to the analysis using the input-output characteristic. We first identify the negative feedback in the system. There is an obvious negative feedback from APC (z variable) on the q and x variables. The term $k_{cdc25basal}(cdc25_{tot} - w)x$ seems to provide an additional negative feedback in the first equation. However, since $k_{cdc25basal} < k_{cdc25}$, combining the two terms gives

$$k_{cdc25}wx + k_{cdc25basal}(cdc25_{tot} - w)x = k_{cdc25basal}cdc25_{tot} + wx(k_{cdc25} - k_{cdc25basal}),$$

which has a positive derivative with respect to w and x. So both w and x increase the production rate of q. Therefore the only negative feedback in the system is caused by the APC degradation of Cdc2-cyclin.

In order to prove that the cell cycle oscillation disappears for weak negative feedback we review the theory linking multivalued input-output characteristics and Morse decompositions developed in [18].

7.2.1. Multivalued characteristics and the global attractor. We consider the system (7.2) as an open loop system

(7.3) $$\dot{X} = F(X, \alpha), \quad z = \bar{h}(X),$$

where we replace the negative feedback $-z$ in the first two equations in (7.2) by a parameter α:

(7.4) $$\dot{q} = k_{synth} + k_{dest}q\alpha - k_{wee1}uq - k_{wee1basal}(wee1_{tot} - u)q + k_{cdc25}w(x - q)$$
$$+ k_{cdc25basal}(cdc25_{tot} - w)(x - q),$$
$$\dot{x} = k_{synth} + k_{dest}x\alpha.$$

In (7.3) we set $X := (q, x, w, u, v, z)$. The output function $\bar{h}$ projects vector X to the z variable. We recover the original system (7.2) as a closed loop system with a negative feedback $\alpha = -z$. The multivalued input-state characteristic $\bar{k}_X(\alpha)$ of (7.3) assigns to each α the set of equilibria of the system, while the input-output characteristic is $\alpha = \bar{k}(\alpha) = -\bar{h}(\bar{k}_X(\alpha))$. In [18] there is an explicit construction of an interval $[a, b] \subset \mathbf{R}$ on the α-axis using the open loop system (7.3) such that the projection of the global attractor of the closed loop system onto the α-axis lies within $[a, b]$. In particular, if this interval is degenerate (i.e., $a = b$), then the long-term behavior of the closed loop system $\dot{X} = F(X, -z)$ is the same as that of the system $\dot{X} = F(X, a)$ at the value $\alpha = a$. We will use this fact below to prove that if the negative feedback is too weak, the cell cycle oscillator stops.

7.2.2. Multivalued characteristic and periodic orbits. We now change (7.2) to the framework discussed in this paper, which is slightly different from the one we have just introduced. We let $x := (q, s, w, u, v)$ and rewrite the system (7.2) as

$$\dot{x} = f(x, -k_{dest}z), \qquad \dot{z} = g(z, v),$$

where the function f comprises the first five equations and $g(z, v)$ is the last equation in (7.2). Since the key parameter affecting the strength of the negative feedback, $k_{dest} = 0.006$, is small, we introduce a new variable, $\zeta := k_{dest}z$. The system becomes

(7.5) $$\dot{x} = f(x, -\zeta), \qquad \dot{\zeta} = k_{dest}g\left(\frac{\zeta}{k_{dest}}, v\right).$$

Even though $k_{dest} \ll 1$, this is not a singular perturbation problem since the function g depends on k_{dest}. We apply the methods developed in this paper to a related class of problems where we rename the first (but not the second) k_{dest} in the last equation by ϵ. We arrive at

(7.6) $$\dot{x} = f(x, -\zeta), \qquad \dot{\zeta} = \epsilon g\left(\frac{\zeta}{k_{dest}}, v\right).$$

Note that while (7.5) is equivalent to (7.2), the system (7.6) is equivalent to (7.2) only when $k_{dest} = \epsilon$. Since the theory developed in this paper is based on singular perturbation theory, when we apply it to (7.6), we will prove the existence of the periodic orbit only for sufficiently small ϵ. Such an argument does not show that the periodic orbit persists all the way to $\epsilon = k_{dest}$, that is, to system (7.5). In fact we will show, using the theory developed in [18],

that when k_{dest} is two orders of magnitude smaller than the value $k_{dest} = 0.006$ listed above, the system (7.2) does not have a periodic orbit. Therefore we conclude that there is an interval of values k_{dest}, that does not contain zero, which is compatible with the existence of the cell cycle oscillation. This suggests that for the proper functioning of the cell cycle the strength of negative feedback cannot be too low or too high.

To study the system (7.6) following the construction leading to (2.6) we construct a model planar system

$$(7.7) \qquad \dot{v} = k^{-1}(v) - \zeta, \qquad \dot{\zeta} = \epsilon g\left(\frac{\zeta}{k_{dest}}, v\right),$$

where $v = k(\zeta)$ is a multivalued input-output characteristic of f in (7.6). To compute $k(\zeta)$ we first compute the input-output characteristic that associates to each ζ the set of equilibria of the system $\dot{x} = f(x, -\zeta)$ in (7.6). The input-output characteristic $k(\zeta)$ is then the value of v on this set of equilibria.

7.2.3. Construction of the characteristics $\bar{k}(\alpha)$ and $k(\zeta)$.
We first compute the equilibria of (7.2) with the first two equations replaced by (7.4). We set the left-hand side of the equations to zero and solve the resulting system to get

$$q = \frac{k_{synth} + k_{cdc25}wx + k_{cdc25basal}(cdc25_{tot} - w)x}{k_{wee1}u + k_{wee1basal}(wee1_{tot} - u) + k_{cdc25}w + k_{cdc25basal}(cdc25_{tot} - w) + k_{dest}\alpha},$$

$$x = \frac{k_{synth}}{k_{dest}\alpha},$$

$$(7.8) \quad w = cdc25_{tot}k_{cdc25on}\frac{q^4}{k_{cdc25off}e_{cdc25}^4 + (k_{cdc25off} + k_{cdc25on})q^4},$$

$$u = wee1_{tot}k_{wee1on}\frac{e_{wee1}^4 + q^4}{k_{wee1on}e_{wee1}^4 + (k_{wee1off} + k_{wee1on})q^4},$$

$$v = plx_{tot}k_{plxon}\frac{q^3}{k_{plxoff}e_{plx}^3 + (k_{plxoff} + k_{plxon})q^3},$$

$$z = apc_{tot}k_{apcon}\frac{v^3}{k_{apcoff}e_{apc}^3 + (k_{apcoff} + k_{apcon})v^3}.$$

Our goal is to compute the output z as a function of α (to get $z = \bar{k}(\alpha)$) and the output v as a function of $\zeta = k_{dest}z = -k_{dest}\alpha$ (to get $v = k(\zeta)$). To this end we insert the second, third, and fourth equations into the first and then solve this equation for q. There are multiple solutions of this equation that correspond to multiple equilibria. It follows that the input-state characteristic is multivalued. To finish the computation we obtain the value of $v = k(\alpha) = k(\zeta/k_{dest})$ by taking the resulting values of q and inserting them into the fifth equation. Finally, we get the value of $z = \bar{k}(\alpha)$ by inserting this value of v into the last equation and computing z. Note that both $\bar{k}$ and k are multivalued as long as the first four equations have multiple solutions for q. We note that these first four equations describe the positive feedback subnetwork consisting of active Cdc2-cyclin (q), total Cdc2-cyclin (y), Cdc25 (w), and Wee1 (u). This clearly shows that the multistability originates from the positive feedback subnetwork.

A

B

C
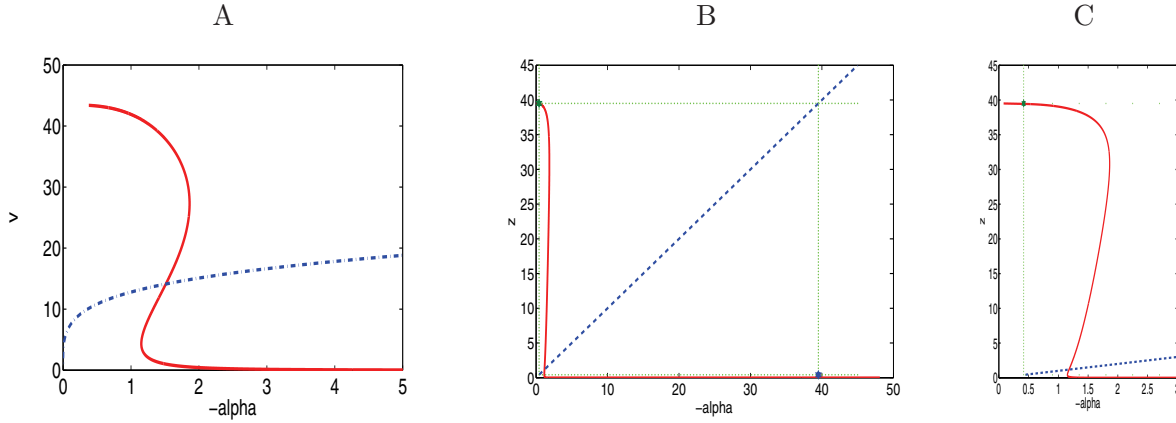
Figure 8. (a) *Two nullclines for the system* (7.7) *in the plane:* $v = k(\alpha)$ *in solid red, and* $g(\alpha, v) = 0$ *in dashed blue.* (b) *The input-output characteristic of* (7.2) *in solid red. The dashed blue curve is the diagonal, and the green dotted square is* $R \times R$ *(see the text). The corresponding periodic orbit is shown in Figure* 7(b). (c) *Detail of* (b)*: the horizontal axis has been rescaled to showcase the multivalued characteristic.*

We will analyze the mutual position of nullclines $v = k(\zeta)$ and $g(\zeta/k_{dest}, v) = 0$ of (7.7) as a function of the parameter k_{dest}. To facilitate this analysis we will use coordinates $(v, \alpha) = (v, \zeta/k_{dest})$ in which the curve $g(\alpha, v) = 0$ does not depend on the parameter k_{dest}.

7.2.4. Results. 1. *The wild type $k_{dest} = 0.006$.* The input-output characteristic $v = k(\zeta) = k(-k_{dest}\alpha)$ and the nullcline $g(v, z) = 0$ of the system (7.6) are shown in Figure 8(a). Notice that in the region $\alpha \in [1.17, 1.85]$ the characteristic $v = k(\alpha)$ is multivalued. Since the nullcline $g(\alpha, v) = 0$ intersects $k(\alpha)$ along the middle branch, Assumption 1 of Theorem 2.2 is satisfied. It is straightforward to check the strong monotonicity of the system (7.6) for a fixed value of α. Since the $k(\alpha)$ has no self-intersections, the function $v = h(x)$ is injective on the set of equilibria. Since linearization of the system of differential equations (7.6) is clearly irreducible, Assumption 2 holds. Since Assumption 3 is generic (except for the stability assumption, which we have checked numerically), we can conclude from Theorem 2.2 that the system (7.6) admits a periodic orbit for sufficiently small ϵ. The simulation of the dynamics of the full system (7.2) suggests that this periodic orbit persists until $\epsilon = k_{dest}$; see Figure 7(b).

In Figure 8(b) we graph an input-output characteristic $\bar{k}(\alpha)$ of (7.2). The projection of the global attractor of (7.2) onto the α variable falls within a bounded closed interval R, which is the base of the green dashed square in Figure 8(b). Since the cubic-like characteristic intersects the diagonal only along the middle branch, the theory developed in [18] shows that there is no nontrivial Morse decomposition (i.e., with more than one Morse set) of the global attractor. This suggests (but does not prove) that the cell cycle periodic orbit is globally stable. A review of the concept of a Morse decomposition can be found in the introduction.

2. $k_{dest} = 0.0006$. We lower k_{dest} by an order of magnitude to $k_{dest} = 0.0006$. The characteristic $k(\alpha)$ shifts to the right; see Figure 9(a). Since $g(\alpha, v) = 0$ still intersects $k(\alpha)$ along the middle branch, we can verify the assumptions of Theorem 2.2 in the same way as above. We conclude from Theorem 2.2 that there is a periodic orbit for (7.6) for sufficiently small ϵ. The simulation of the dynamics of the full system (7.2) again shows that this periodic
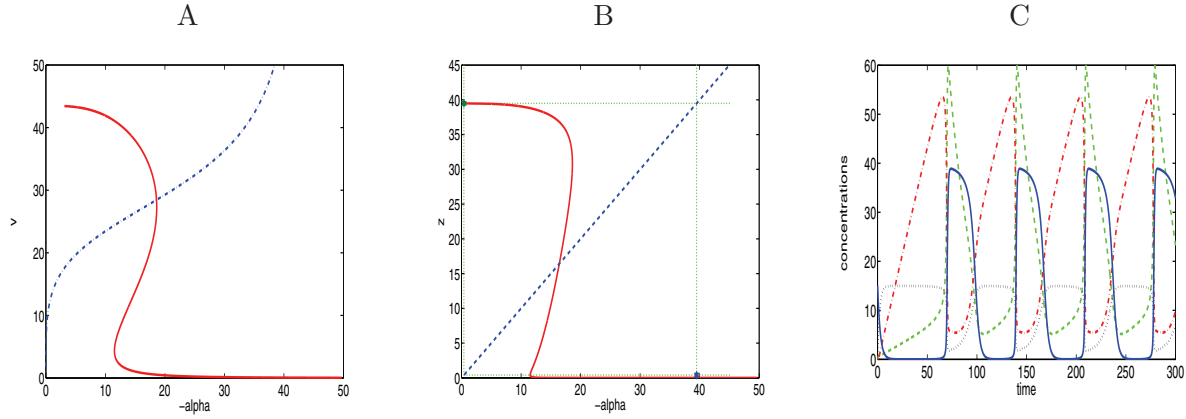
Figure 9. (a) *Two nullclines of the planar system* (7.7). (b) *The input-output characteristic of the model with $k_{dest} = 0.0006$. The dashed curve is the diagonal.* (c) *The corresponding dynamics. The color legend is the same as in Figure* 8.
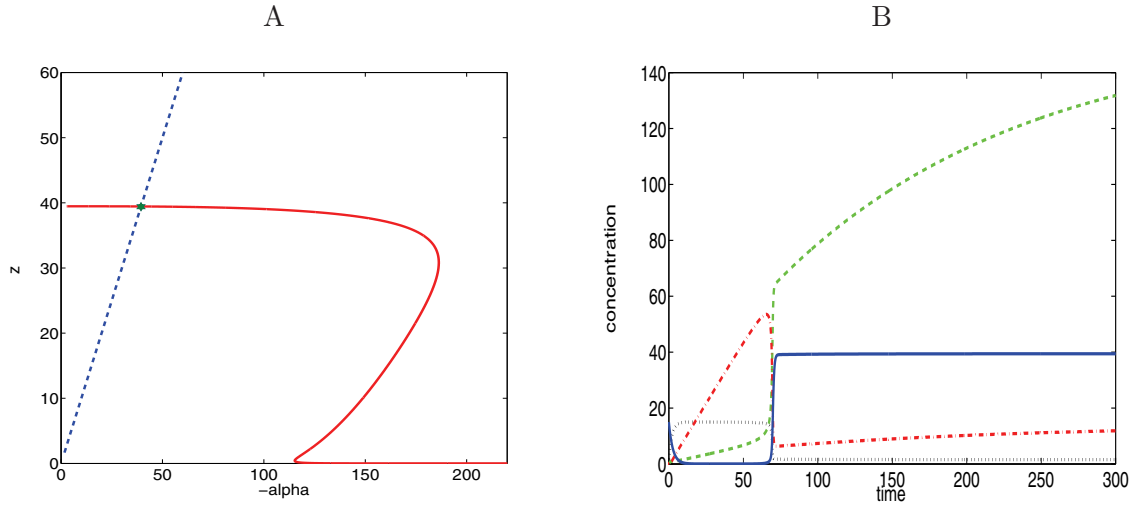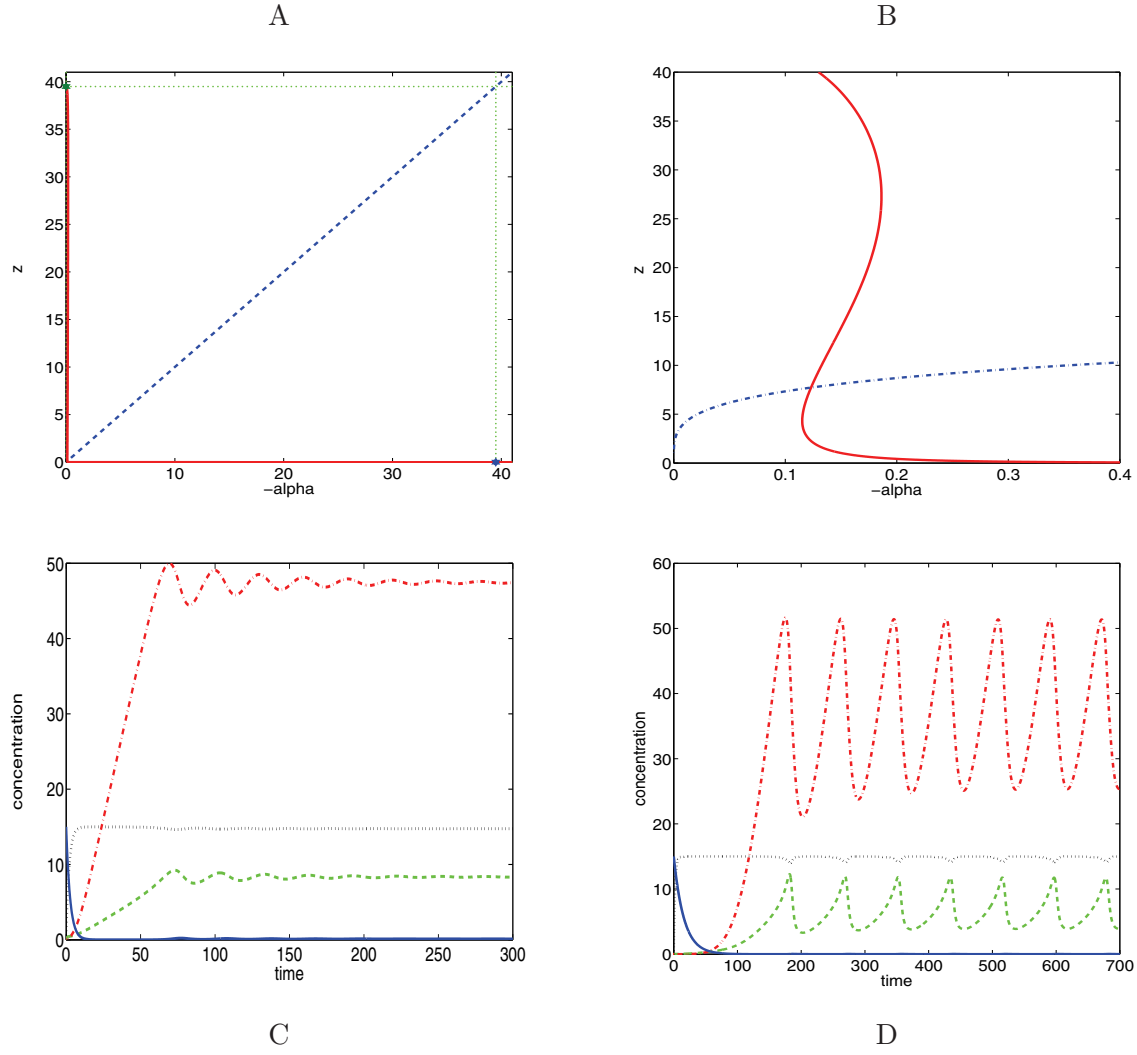

Figure 10. (a) *The input-output characteristic $\bar{k}$ of the model with $k_{dest} = 0.00006$. The legend is the same as in Figure* 8. (b) *The corresponding dynamics. The color legend is the same as in Figure* 7.

orbit persists until $\epsilon = k_{dest}$; see Figure 9(c). The input-output characteristic $\bar{k}(\alpha)$ and the global projection interval (dashed square in Figure 9(b)) suggest that all solutions converge to this periodic orbit.

We also note that the characteristic Figure 9(a) has a larger α projection than that in Figure 8(a). Since the periodic orbit should be a relaxation orbit on this nullcline, we expect gentler oscillations in the dynamics. This is confirmed by comparing Figures 7(b) and 9(c).

3. $k_{dest} = 0.00006$. We lower k_{dest} another order of magnitude to $k_{dest} = 0.00006$. In Figure 10(a) we graph the characteristic $\bar{k}(\alpha)$ and the interval in α that contains the projection of the global attractor. This interval is degenerate and contains a single value $\alpha_0 = -z_0 \approx 39.5$. This value is the projection of the intersection of the diagonal and the characteristic along the

A   B

C   D

Figure 11. $k_{dest} = 0.06$: (a) *input-output characteristic $\bar{k}(\alpha)$; (b) the intersections of the nullclines is along the middle branch; (c) the system (7.2) does not exhibit oscillations; (d) oscillations are recovered in system (7.6) for $\epsilon = 0.01$. The color code in (a) and (b) matches that of Figure 8, and in (c) and (d) it matches that of Figure 7.*

upper branch. The theory in [18] predicts global convergence to an equilibrium with the value of $z = z_0$. This is confirmed by a numerical simulation of the dynamics of (7.2) in Figure 10(b). There is no cell cycle periodic orbit in (7.2) for $k_{dest} = 0.00006$.

4. $k_{dest} = 0.06$. In this case the bistability in $\bar{k}(\alpha)$ occurs in a very narrow range $\alpha \in [0.116, 0.185]$, which on the scale of Figure 11(a) can be seen as a vertical line on the left side of the picture. However, the attracting square contains this bistable region (Figure 11(a)), and the nullclines $k(\alpha)$ and $g(z, v) = 0$ intersect along the middle branch of $k(\alpha)$; see Figure 11(b). As before, by Theorem 2.2 the system (7.6) has a periodic orbit for ϵ small enough. However, numerical simulation of the system (7.2) shows the convergence to an equilibrium (Figure

11(c)). This case illustrates the gap between systems (7.6) and (7.2) and the limitations of the singular perturbation argument. In Figure 11(d) we find the periodic orbit when we set $\epsilon = 0.01$ in (7.6), which does not persist until $\epsilon = k_{dest} = 0.06$ (Figure 11(c)). This confirms that for strong negative feedback (high values of k_{dest}) the relationship between the dynamics of (7.2) and the nullclines $k(\alpha)$ and $g(z, v) = 0$ disappears.

8. Conclusions. We have developed a new theory based on multivalued input-output characteristics that can be used to provide a rigorous proof of the existence of relaxation periodic orbits in monotone systems coupled to a scalar differential equation providing a negative feedback. Our construction can be used to prove the existence of periodic orbits in slow-fast systems of arbitrary dimension.

We applied our theory to a model of a cell cycle in *Xenopus* embryos. Abrupt changes in signals upon entry to mitosis suggest that the cell cycle is generated by a relaxation oscillation. Our results show that the cell cycle orbit is not a relaxation oscillator. However, we construct a closely related system that exhibits relaxation oscillations and that approximates the cell cycle oscillator for an intermediate range of negative feedback strengths. We show that the cell cycle oscillation disappears if the negative feedback is too weak or too strong.

REFERENCES

[1] B. ALBERTS, A. JOHNSON, J. LEWIS, M. RAFF, K. ROBERTS, AND P. WALTER, *Molecular Biology of the Cell*, 4th ed., Garland Science, Taylor & Francis Group, London, 2002.

[2] D. ANGELI AND E. D. SONTAG, *Monotone control systems*, IEEE Trans. Automat. Control, 48 (2003), pp. 1684–1698.

[3] D. ANGELI AND E. D. SONTAG, *Multi-stability in monotone input/output systems*, Systems Control Lett., 51 (2004), pp. 185–202.

[4] D. ANGELI, J. E. FERRELL, JR., AND E. SONTAG, *Detection of multistability, bifurcations, and hysteresis in a large class of biological positive-feedback systems*, Proc. Natl. Acad. Sci. USA, 101 (2004), pp. 1822–1827.

[5] C. P. BAGOWSKI AND J. E. FERRELL, JR., *Bistability in the JNK cascade*, Curr. Biol., 11 (2001), pp. 1176–1182.

[6] U. S. BHALLA, P. T. RAM, AND R. IYENGAR, *MAP kinase phosphatase as a locus of flexibility in a mitogen-activated protein kinase signaling network*, Science, 297 (2002), pp. 1018–1023.

[7] P. BRUNOVSKÝ, *Controlling nonuniqueness of local invariant manifolds*, J. Reine Angew. Math., 446 (1994), pp. 115–135.

[8] A. CILIBERTO AND J. TYSON, *Mathematical model for early development of the sea urchin embryo*, Bull. Math. Biol., 62 (2000), pp. 37–59.

[9] C. CONLEY, *Isolated Invariant Sets and the Morse Index*, CBMS Regional Conf. Ser. in Math. 38, AMS, Providence, RI, 1978.

[10] P. DE LEENHEER AND M. MALISOFF, *A small-gain theorem for monotone systems with multi-valued input-state characteristics*, IEEE Trans. Automat. Control, 51 (2006), pp. 287–292.

[11] M. B. ELOWITZ AND S. LEIBLER, *A synthetic oscillatory network of transcriptional regulators*, Nature, 403 (2000), pp. 335–338.

[12] G. ENCISO AND E. D. SONTAG, *Monotone systems under positive feedback: Multistability and a reduction theorem*, Systems Control Lett., 54 (2005), pp. 159–168.

[13] G. ENCISO AND E. D. SONTAG, *Global attractivity, I/O monotone small-gain theorems, and biological delay systems*, Discrete Contin. Dyn. Syst., 14 (2006), pp. 549–578.

[14] G. A. ENCISO AND E. D. SONTAG, *Monotone bifurcation graphs*, J. Biol. Dyn., 2 (2008), pp. 121–139.

[15] G. ENCISO, H. L. SMITH, AND E. D. SONTAG, *Nonmonotone systems decomposable into monotone systems with negative feedback*, J. Differential Equations, 224 (2006), pp. 205–227.

[16] J. E. FERRELL, *Self-perpetuating states in signal transduction: Positive feedback, double-negative feedback and bistability*, Curr. Opin. Cell Biol., 14 (2002), pp. 140–148.

[17] J. E. FERRELL AND E. M. MACHLEDER, *The biochemical basis of an all-or-none cell fate switch in Xenopus oocytes*, Science, 280 (1998), pp. 895–898.

[18] T. GEDEON AND W. HINES, *Multi-valued characteristics and Morse decompositions*, J. Differential Equations, 247 (2009), pp. 1013–1042.

[19] T. GEDEON AND E. D. SONTAG, *Oscillations in multi-stable monotone systems with slowly varying feedback*, J. Differential Equations, 239 (2007), pp. 273–295.

[20] M. GOLUBITSKY AND D. SCHAEFFER, *Singularities and Groups in Bifurcation Theory*, Springer-Verlag, New York, 1984.

[21] J. K. HALE, *Ordinary Differential Equations*, 2nd ed., Krieger, Huntington, NY, 1980.

[22] J. HASTY, M. DOLNIK, V. ROTTSCHAFER, AND J. J. COLLINS, *Synthetic gene network for entraining and amplifying cellular oscillations*, Phys. Rev. Lett., 88 (2002), article 148101.

[23] A. KATOK AND B. HASSELBLATT, *Introduction to the Modern Theory of Dynamical Systems*, Cambridge University Press, Cambridge, UK, 1995.

[24] S. LEFSCHETZ, *Differential Equations: Geometric Theory*, Dover, New York, 1977.

[25] J. LEWIS, *From signals to patterns: Space, time, and mathematics in developmental biology*, Science, 322 (2008), pp. 399–403.

[26] CH. MCCORD, K. MISCHAIKOW, AND M. MROZEK, *Zeta functions, periodic trajectories, and the Conley index*, J. Differential Equations, 121 (1995), pp. 258–292.

[27] D. O. MORGAN, *The Cell Cycle: Principles of Control*, Primers in Biology, New Science Press, London, 2007.

[28] A. NOVICK AND M. WIENER, *Enzyme induction as an all-or-none phenomenon*, Proc. Natl. Acad. Sci. USA, 43 (1957), pp. 553–566.

[29] B. NOVAK AND J. J. TYSON, *Numerical analysis of a comprehensive model of M-phase control in Xenopus oocyte extracts and intact embryos*, J. Cell Sci., 106 (1993), pp. 1153–1168.

[30] P. NURSE, *Universal control mechanism regulating the onset of the M-phase*, Nature, 344 (1990), pp. 503–508.

[31] J. R. POMERENING, E. D. SONTAG, AND J. R. FERRELL, JR., *Building a cell cycle oscillator: Hysteresis and bistability in the activation of Cdc2*, Nat. Cell Biol., 5 (2003), pp. 346–351.

[32] J. R. POMERENING, S. Y. KIM, AND J. E. FERRELL, JR., *Systems-level dissection of the cell-cycle oscillator: Bypassing positive feedback produces damped oscillations*, Cell, 122 (2005), pp. 565–578.

[33] M. PTASHNE, *A Genetic Switch: Phage Lambda and Higher Organisms*, Cell Press, Blackwell Scientific, Cambridge, MA, 1992.

[34] W. SHA, J. MOORE, K. CHEN, Y. D. LASSALETTA, C. S. YI, J. J. TYSON, AND I. C. SIBLE, *Hysteresis drives cell-cycle transitions in Xenopus laevis egg extracts*, Proc. Natl. Acad. Sci. USA, 100 (2003), pp. 975–980.

[35] H. SMITH, *Monotone Dynamical Systems*, Math. Surveys Monogr. 41, AMS, Providence, RI, 1995.

[36] J. STRICKER, S. COOKSON, M. R. BENNETT, W. H. MATHER, L. S. TSIMRING, AND J. HASTY, *A fast, robust and tunable synthetic gene oscillator*, Nature, 456 (2008), pp. 516–520.

[37] J. J. TYSON, A. CSIKASZ-NAGY, AND B. NOVAK, *The dynamics of cell cycle regulation*, BioEssays, 24 (2002), pp. 1095–1109.